

# CASE FILE COPY

## NATIONAL ADVISORY COMMITTEE FOR AERONAUTICS

TECHNICAL NOTE 2310

GENERALIZATION OF BOUNDARY-LAYER MOMENTUM-INTEGRAL  
EQUATIONS TO THREE-DIMENSIONAL FLOWS INCLUDING  
THOSE OF ROTATING SYSTEM

By Artur Mager

Lewis Flight Propulsion Laboratory  
Cleveland, Ohio



Washington

March 1951

RELEASE DATE

JUL 30 1952

ERRATA No. 1

NACA TN 2310

GENERALIZATION OF BOUNDARY-LAYER MOMENTUM-INTEGRAL  
EQUATIONS TO THREE-DIMENSIONAL FLOWS INCLUDING  
THOSE OF ROTATING SYSTEM

By Artur Mager

March 1951

Page 24, equation (35c) and page 25, equation (37): The quantity

$$\left[ (1+H)c - H \frac{2\omega_y}{U} \right] \quad \text{should be} \quad \left[ (1+H)c + H \frac{2\omega_y}{U} \right]$$

NATIONAL ADVISORY COMMITTEE FOR AERONAUTICS

TECHNICAL NOTE 2310

GENERALIZATION OF BOUNDARY-LAYER MOMENTUM-INTEGRAL EQUATIONS TO  
THREE-DIMENSIONAL FLOWS INCLUDING THOSE OF ROTATING SYSTEM

By Artur Mager

SUMMARY

The Navier-Stokes equations of motion and the equation of continuity are transformed so as to apply to an orthogonal curvilinear coordinate system rotating with a uniform angular velocity about an arbitrary axis in space. A usual simplification of these equations as consistent with the accepted boundary-layer theory and an integration of these equations through the boundary layer result in boundary-layer momentum-integral equations for three-dimensional flows that are applicable to either rotating or nonrotating fluid boundaries.

These equations are simplified and an approximate solution in closed integral form is obtained for a generalized boundary-layer momentum-loss thickness and flow deflection at the wall in the turbulent case.

A numerical evaluation of this solution carried out for data obtained in a curving nonrotating duct shows a fair quantitative agreement with the measured values.

The form in which the equations are presented is readily adaptable to cases of steady, three-dimensional, incompressible boundary-layer flow like that over curved ducts or yawed wings and it also may be used to describe the boundary-layer flow over various rotating surfaces, thus applying to turbomachinery, propellers, and helicopter blades.

INTRODUCTION

The development of the boundary layer on the various parts of turbomachinery (compressors and turbines), helicopter blades, propellers, and in curved ducts is influenced by centrifugal and Coriolis forces in addition to the pressure and viscous forces. As a result of these forces, the flow in the boundary layer not only has the characteristic velocity deficiency but also has, because of this velocity deficiency, direction different from that of the flow outside the

boundary layer. Thus the behavior of the boundary layer in three-dimensional flow may be quite unlike the behavior in two-dimensional flow. The effect of these additional forces on the boundary layer has been realized for some time and the observed discrepancies in the boundary-layer behavior have usually been explained only in a qualitative manner as, for instance, in references 1 to 4.

The literature concerning the theoretical aspect of the three-dimensional boundary-layer flow is meager. For the laminar case most of the published work has been carried out in connection with the yawed wing (references 5 to 7). For the turbulent case, although a number of researchers have established the general form of the differential equations applicable, no actual solutions of these equations have been obtained. Tetervin, for instance, presents boundary-layer momentum-integral equations in three dimensions for a fluid of variable density and viscosity (reference 8). Gruschwitz establishes the momentum-integral equations for boundary-layer flow along an arbitrarily curved streamline in reference 9. Burgers gives the differential equations on the development of boundary layers in the case of axially symmetric flows having a rotational component (reference 10). Prandtl, in addition to presenting a form of three-dimensional momentum-integral equations, suggests the general procedure that could be followed to obtain a solution (reference 11). Experimental data are similarly lacking. In spite of considerable literature search, only the data of Gruschwitz (reference 9) for a curved duct and the data of Kuethe, McKee, and Curry (reference 12) for a yawed wing were found.

As a result of research on this problem at the NACA Lewis laboratory, the boundary-layer momentum-integral equations are derived and presented herein for a set of orthogonal curvilinear coordinates, which may or may not be rotating about an arbitrary axis in space and can be laid out along a streamline of the potential flow. The so generalized equations are then transformed by use of an assumed velocity distribution and friction law for turbulent boundary layer so that an approximate solution can be obtained for the boundary-layer momentum thickness and the direction of boundary-layer flow. Finally, a numerical solution is carried out for the Gruschwitz data in order to make a comparison between the estimated and actual measured values.

The equations as given in their generalized form are readily adaptable to cases of steady, three-dimensional, incompressible boundary-layer flow, involving centrifugal and Coriolis forces. The approximate solution, however, has been carried out only for the turbulent boundary layer, because in most of the aerodynamic configurations, where these equations apply, transition from laminar to turbulent flow occurs

comparatively early in the flow process. A laminar form of the approximate solution can be obtained by simple substitution of a suitable velocity profile and friction law.

It should be noted that whereas the differential equations describe the flow phenomena with only the accepted simplifications, the approximate solution depends to some extent on the assumed boundary-layer velocity profiles and the relation for friction. Both of these assumptions were made on the basis of the data of Gruschwitz (reference 9) only, because the data of reference 12 were not adaptable to extensive computations for the purpose of this analysis. The measurements of Gruschwitz, on the other hand, have certain shortcomings as they were obtained in a nonrotating channel formed by two circular-arc shaped walls. Thus the generality of the velocity profiles measured by Gruschwitz is in question. A revision of the approximate solution can therefore be expected when more data become available. In addition, any speculation on the occurrence of boundary-layer separation (which by definition is a special form of a velocity profile) would be absolutely meaningless; no further mention will therefore be made of this phase of the problem.

#### SYMBOLS

The following symbols are used in this report (the dimensions are given in right-hand column):

|             |  |               |
|-------------|--|---------------|
| A           | constant occurring in second approximation for $\Theta$      | ( $l^{-1}$ )  |
| $\bar{a}$   | resultant acceleration vector in fixed (inertial) system     | ( $lt^{-2}$ ) |
| $\bar{a}_0$ | resultant acceleration vector in Cartesian coordinate system | ( $lt^{-2}$ ) |
| B           | constant occurring in second approximation for $\Theta$      | (0)           |
| $\bar{b}$   | position vector of particle                                  | ( $l$ )       |
| c           | curvature of x-axis (fig. 1), $\frac{d\beta}{dx}$            | ( $l^{-1}$ )  |
| d           | constant $\geq \delta$                                       | ( $l$ )       |

$$E_1(x) = e^{\left( \frac{0.01255}{(K-J)} \int_{x_1}^x \frac{dx}{\Theta_I} \right)} \quad (0)$$

$$E_2(x) = e^{\left( \frac{J}{4} \int_{x_1}^x c \epsilon \, dx \right)} \quad (0)$$

$$E_3(x) = e^{\left( \frac{18}{4} J \int_{x_1}^x \epsilon \frac{\omega_y}{U} \, dx \right)} \quad (0)$$

$e_{xx}, e_{xy} \dots$  rate-of-strain components ( $t^{-1}$ )

$F$  resultant-force vector acting on particle ( $mlt^{-2}$ )

$f_X, f_Y, f_Z$  components of body forces per unit mass ( $lt^{-2}$ )

$G$  function describing boundary-layer velocity profile,  
also taken as  $\left( \frac{y}{\delta} \right)^{\frac{1}{n}}$  (0)

$g$  function describing boundary-layer velocity profile,  
also taken as  $\left( 1 - \frac{y}{\delta} \right)^2$  (0)

$H, J, K, L$  quantities describing relations among various characteristic loss thicknesses in boundary layer (0)

$h_1, h_2, h_3$  transformation coefficients (0)

$l$  length

$MN$  parameter determining nature of boundary-layer equations (0)

$m$  mass

$P$  static pressure ( $ml^{-1}t^{-2}$ )

$P_{XX}, P_{YY}, \dots$  components of stress per unit area in Cartesian coordinate system ( $ml^{-1}t^{-2}$ )

|                             |   |             |
|-----------------------------|---|-------------|
| $\bar{q}_0$                 | resultant velocity vector   | $(lt^{-1})$ |
| R                           | perpendicular distance of particle from axis of rotation  | $(l)$       |
| $R(\theta_x)$               | Reynolds number based on $\theta_x$ , $\frac{\theta_x U}{\nu}$  | $(0)$       |
| r                           | radius of circle  | $(l)$       |
| S                           | total path length $\int_0^S dx$   | $(l)$       |
| s                           | arc length  | $(l)$       |
| t                           | time  |             |
| U,V,W                       | values of u, v, and w outside boundary layer  | $(lt^{-1})$ |
| $U_0, V_0, W_0$             | velocities in Cartesian coordinate system   | $(lt^{-1})$ |
| u,v,w                       | time averaged velocities in curvilinear coordinate system   | $(lt^{-1})$ |
| X,Y,Z                       | Cartesian coordinate system   | $(l)$       |
| x,y,z                       | orthogonal curvilinear coordinate system  | $(l)$       |
| $Z_1(x)$                    | function used in transformation   | $(l)$       |
| $\alpha$                    | boundary-layer deflection angle measured from direction of resultant skin-friction stress to direction of flow outside boundary layer | $(0)$       |
| $\beta$                     | angle between X-axis and tangent to x-axis  | $(0)$       |
| $\delta$                    | boundary-layer thickness  | $(l)$       |
| $\delta_x^*, \delta_z^*$    | displacement thicknesses in three-dimensional boundary layer  | $(l)$       |
| $\epsilon$                  | measure of boundary-layer deflection, $\tan \alpha$   | $(0)$       |
| $\zeta_p, \zeta_+, \zeta_-$ | slope of characteristic line  | $(0)$       |

|  |  |   |
|--|--|---|
| $\Theta$                                       | generalized boundary-layer momentum-loss thickness,<br>$\theta_{xR}^{1/4}(\theta_x)$ | (l)   |
| $\theta_x, \theta_z, \theta_{xz}, \theta_{zx}$ | momentum-loss thicknesses in three-dimensional boundary layer                        | (l)   |
| $\lambda$                                      | variable of function $\psi$ , $\left(z - J \int_{x_i}^x \epsilon \, dx\right)$       | (l)   |
| $\nu$  | kinematic viscosity  | (l <sup>2</sup> t <sup>-1</sup> )   |
| $\xi, \eta, \zeta$                             | components of vorticity vector   | (t <sup>-1</sup> )  |
| $\rho$   | density  | (ml <sup>-3</sup> )   |
| $\sigma_x, \tau_{xy} \dots$                    | apparent stresses existing in turbulent flow   | (ml <sup>-1</sup> t <sup>-2</sup> )   |
| $\tau_o$                                       | shear stress at wall   | (ml <sup>-1</sup> t <sup>-2</sup> )   |
| $\psi$   | arbitrary function satisfying equation (39) and boundary conditions                  | $\left( \left[ \frac{(5H+9)}{4} + 1 \right]_t \left[ \frac{-(5H+9)}{4} \right] \right)$ |
| $\omega$                                       | angular velocity   | (t <sup>-1</sup> )  |
| $\omega_x, \omega_y, \omega_z$                 | components of vector $\omega$ in Cartesian coordinate system                         | (t <sup>-1</sup> )  |
| $\omega_x, \omega_y, \omega_z$                 | components of vector $\omega$ in curvilinear coordinate system                       | (t <sup>-1</sup> )  |
| Subscripts:                                    |  |   |
| i  | initial value  |   |
| x  | x-direction  |   |
| z  | z-direction  |   |
| I, II  | order of approximations  |   |

For Gruschwitz data-point designations and streamline designations, see figure 2.



## DERIVATION OF BOUNDARY-LAYER MOMENTUM-INTEGRAL EQUATIONS

The equations for steady flow of a fluid having constant density are derived in a Cartesian coordinate system  $X, Y, Z$ , rotating with uniform angular velocity about an arbitrary axis in space. These equations are then transformed to an orthogonal curvilinear coordinate system  $x, y, z$ , such that the  $x$ -axis can be placed along any convenient path in the  $XY$ -plane, which is considered as a plane of a wall. These equations are then simplified in a manner consistent with the boundary-layer theory. If the path is chosen so as to match a streamline of the potential flow, only one velocity will exist outside the boundary layer, that along the streamline. Furthermore, the changes in boundary-layer quantities in a direction other than that along the streamline are expected to be relatively small in comparison to the changes along the streamline. Additional simplifications may thus be possible. Finally, integration through the boundary layer gives the generalized form of momentum-integral equations for three-dimensional flows that may or may not involve rotation of the system.

Equations for steady flow of fluid with constant density in rotating Cartesian coordinate system. - The Navier-Stokes equations of flow for a fixed Cartesian coordinate system  $X, Y, Z$  (reference 13, p. 576) are

$$\rho \frac{DU_o}{Dt} = \rho f_X + \frac{\partial p_{XX}}{\partial X} + \frac{\partial p_{YX}}{\partial Y} + \frac{\partial p_{ZX}}{\partial Z} \quad (1a)$$

$$\rho \frac{DV_o}{Dt} = \rho f_Y + \frac{\partial p_{XY}}{\partial X} + \frac{\partial p_{YY}}{\partial Y} + \frac{\partial p_{ZY}}{\partial Z} \quad (1b)$$

$$\rho \frac{DW_o}{Dt} = \rho f_Z + \frac{\partial p_{XZ}}{\partial X} + \frac{\partial p_{YZ}}{\partial Y} + \frac{\partial p_{ZZ}}{\partial Z} \quad (1c)$$

and the equation of continuity is

$$\frac{\partial U_o}{\partial X} + \frac{\partial V_o}{\partial Y} + \frac{\partial W_o}{\partial Z} = 0 \quad (2)$$

It is now assumed that this Cartesian coordinate system is rotating with a uniform angular velocity  $\omega$  and that the observations of the motion of the fluid particles are still made from a position rigidly attached to the same system. The velocity  $\bar{q}_o$  and acceleration  $\bar{a}_o$  are as seen by the observer, that is, they are relative to the  $X, Y, Z$  system. Because of the rotation, however, the  $X, Y, Z$  system is not an inertial system (reference 14, p. 53) and thus the second law of motion holds only with respect to acceleration  $\bar{a}$  relative to some other system that is nonrotating,

$$m\bar{a} = F$$

In terms of  $\bar{a}_0$  then (reference 14, p. 104),

$$m\bar{a}_0 + m\omega \times (\omega \times \bar{b}) + 2m\omega \times \bar{q}_0 = F$$

Here  $m\omega \times (\omega \times \bar{b})$  represents the centrifugal force and  $2m\omega \times \bar{q}_0$  is the Coriolis force.

Thus for a Cartesian coordinate system rotating with a uniform angular velocity  $\omega$ , the expressions for  $\frac{DU_0}{Dt}$ ,  $\frac{DV_0}{Dt}$ , and  $\frac{DW_0}{Dt}$  must be modified by proper components of the Coriolis and centrifugal accelerations. For steady flow, the component accelerations as referred to a rotating Cartesian coordinate system are therefore

$$\frac{DU_0}{Dt} = U_0 \frac{\partial U_0}{\partial X} + V_0 \frac{\partial U_0}{\partial Y} + W_0 \frac{\partial U_0}{\partial Z} + 2(\omega_Y W_0 - \omega_Z V_0) - \omega^2 R \frac{\partial R}{\partial X} \quad (3a)$$

$$\frac{DV_0}{Dt} = U_0 \frac{\partial V_0}{\partial X} + V_0 \frac{\partial V_0}{\partial Y} + W_0 \frac{\partial V_0}{\partial Z} + 2(\omega_Z U_0 - \omega_X W_0) - \omega^2 R \frac{\partial R}{\partial Y} \quad (3b)$$

$$\frac{DW_0}{Dt} = U_0 \frac{\partial W_0}{\partial X} + V_0 \frac{\partial W_0}{\partial Y} + W_0 \frac{\partial W_0}{\partial Z} + 2(\omega_X V_0 - \omega_Y U_0) - \omega^2 R \frac{\partial R}{\partial Z} \quad (3c)$$

The equation of continuity, which does not involve any accelerations, remains the same.

Transformation to orthogonal curvilinear coordinate system. - Transformations similar to those of Gruschwitz (reference 9) are used as indicated in figure 1 with the precaution that the system remain right-handed.

$$\left. \begin{aligned} X &= \int_0^x \cos \beta \, dx + z \sin \beta \\ Y &= y \\ Z &= Z_1 + z \cos \beta \end{aligned} \right\} \quad (4)$$

where

$$Z_1 = \text{constant} - \int_0^x \sin \beta \, dx$$

and

$$\beta = \beta(x)$$

Use of these transformations permits an arbitrary curvature of the x-axis in only one plane, the XZ-plane. Thus the solution is somewhat restricted. In two-dimensional boundary-layer investigations, however, it is found that the boundary-layer equations are unaffected if the radius of curvature in the XY-plane is large as compared with the boundary-layer thickness (reference 15, p. 120). In three-dimensional boundary layer the same limitation will probably apply providing, of course, the values of  $\omega_x$ ,  $\omega_y$ , and  $\omega_z$  are properly adjusted to take care of this additional curvature. Setting

$$c = \frac{d\beta}{dx} \quad (\text{curvature of x-axis})$$

gives

$$\begin{array}{lll} \frac{\partial X}{\partial x} = (1+cz) \cos \beta & \frac{\partial X}{\partial y} = 0 & \frac{\partial X}{\partial z} = \sin \beta \\ \frac{\partial Y}{\partial x} = 0 & \frac{\partial Y}{\partial y} = 1 & \frac{\partial Y}{\partial z} = 0 \\ \frac{\partial Z}{\partial x} = -(1+cz) \sin \beta & \frac{\partial Z}{\partial y} = 0 & \frac{\partial Z}{\partial z} = \cos \beta \end{array}$$

The elements of length at  $(x,y,z)$  in the direction of the increasing coordinates are (reference 15, p. 101):

$$h_1 dx, \quad h_2 dy, \quad h_3 dz$$

Thus,

$$(ds)^2 = (h_1)^2 (dx)^2 + (h_2)^2 (dy)^2 + (h_3)^2 (dz)^2 = (dx)^2 + (dy)^2 + (dz)^2$$

But because

$$dX = \frac{\partial X}{\partial x} dx + \frac{\partial X}{\partial y} dy + \frac{\partial X}{\partial z} dz$$

and so forth,

$$(ds)^2 = (1+cz)^2 (dx)^2 + (dy)^2 + (dz)^2$$

and

$$h_1 = (1+cz) \quad h_2 = 1 \quad h_3 = 1 \quad (5)$$

The expressions for the linear accelerations can be written directly, as given in reference 13 (p. 158). (It should be noted that the  $h$  values herein are reciprocals of those in reference 13.) The components of a gradient now are

$$\frac{1}{h_1} \frac{\partial}{\partial x} \quad \frac{1}{h_2} \frac{\partial}{\partial y} \quad \frac{1}{h_3} \frac{\partial}{\partial z}$$

whereas the components of  $\bar{q}_0 \times \omega$  remain

$$V\omega_z - W\omega_y \quad W\omega_x - U\omega_z \quad U\omega_y - V\omega_x$$

Thus the accelerations in the rotating  $x, y, z$  system are written as

$$\begin{aligned} \frac{DU}{Dt} = & \frac{U}{h_1} \frac{\partial U}{\partial x} + \frac{V}{h_2} \frac{\partial U}{\partial y} + \frac{W}{h_3} \frac{\partial U}{\partial z} + \frac{V}{h_1 h_2} \left( U \frac{\partial h_1}{\partial y} - V \frac{\partial h_2}{\partial x} \right) + \frac{W}{h_1 h_3} \left( U \frac{\partial h_1}{\partial z} - W \frac{\partial h_3}{\partial x} \right) + \\ & 2(\omega_y W - \omega_z V) - \frac{1}{h_1} \omega^2 R \frac{\partial R}{\partial x} \end{aligned}$$

And the expressions for  $\frac{DV}{Dt}$  and  $\frac{DW}{Dt}$  follow from symmetry. The equation for the divergence now has the form

$$\text{div } \bar{q}_0 = \frac{1}{h_1 h_2 h_3} \left[ \frac{\partial}{\partial x} (h_2 h_3 U) + \frac{\partial}{\partial y} (h_3 h_1 V) + \frac{\partial}{\partial z} (h_1 h_2 W) \right] = 0$$

Whereas the components of the curl  $\bar{q}_0$  are

$$\begin{aligned} \xi &= \frac{1}{h_2 h_3} \left[ \frac{\partial}{\partial y} (h_3 W) - \frac{\partial}{\partial z} (h_2 V) \right] \\ \eta &= \frac{1}{h_3 h_1} \left[ \frac{\partial}{\partial z} (h_1 U) - \frac{\partial}{\partial x} (h_3 W) \right] \\ \zeta &= \frac{1}{h_1 h_2} \left[ \frac{\partial}{\partial x} (h_2 V) - \frac{\partial}{\partial y} (h_1 U) \right] \end{aligned}$$

In order to obtain the viscous terms the preceding expressions are used in the expansion of

$$v \left[ \text{grad} (\text{div } \bar{q}_0) - \text{curl} (\text{curl } \bar{q}_0) \right]$$

If equations (5) are substituted into these general expressions and the differentiations are carried out, the equations for flow in orthogonal curvilinear coordinate system rotating with an angular velocity  $\omega$  are obtained. The body forces are neglected here.

$$\begin{aligned} & \frac{U}{1+zc} \frac{\partial U}{\partial x} + v \frac{\partial U}{\partial y} + w \frac{\partial U}{\partial z} + \frac{c}{1+zc} UW - \frac{1}{1+zc} \omega^2 R \frac{\partial R}{\partial x} + 2(\omega_y W - \omega_z V) \\ &= - \frac{1}{1+cz} \frac{1}{\rho} \frac{\partial P}{\partial x} + v \left[ \frac{1}{(1+cz)^2} \frac{\partial^2 U}{\partial x^2} - \frac{z}{(1+cz)^3} \frac{\partial U}{\partial x} \frac{dc}{dx} + \frac{\partial^2 U}{\partial y^2} + \right. \\ & \quad \left. \frac{\partial^2 U}{\partial z^2} + \frac{c}{1+cz} \frac{\partial U}{\partial z} - \frac{Uc^2}{(1+cz)^2} + \frac{W}{(1+cz)^3} \frac{dc}{dx} + \frac{2c}{(1+cz)^2} \frac{\partial W}{\partial x} \right] \end{aligned} \quad (6a)$$

$$\begin{aligned} & U \frac{\partial V}{\partial x} + v \frac{\partial V}{\partial y} + w \frac{\partial V}{\partial z} - \frac{1}{1+zc} \omega^2 R \frac{\partial R}{\partial y} + 2(\omega_z U - \omega_x W) = - \frac{1}{\rho} \frac{\partial P}{\partial y} + \\ & v \left[ \frac{1}{(1+cz)^2} \frac{\partial^2 V}{\partial x^2} - \frac{z}{(1+cz)^3} \frac{\partial V}{\partial x} \frac{dc}{dx} + \frac{\partial^2 V}{\partial y^2} + \frac{\partial^2 V}{\partial z^2} + \frac{c}{1+cz} \frac{\partial V}{\partial z} \right] \end{aligned} \quad (6b)$$

$$\begin{aligned} & \frac{U}{1+zc} \frac{\partial W}{\partial x} + v \frac{\partial W}{\partial y} + w \frac{\partial W}{\partial z} - \frac{c}{1+zc} U^2 - \omega^2 R \frac{\partial R}{\partial z} + 2(\omega_x V - \omega_y U) = - \frac{1}{\rho} \frac{\partial P}{\partial z} + \\ & v \left[ \frac{1}{(1+cz)^2} \frac{\partial^2 W}{\partial x^2} - \frac{U}{(1+cz)^3} \frac{dc}{dx} - \frac{z}{(1+cz)^3} \frac{\partial W}{\partial x} \frac{dc}{dx} + \right. \\ & \quad \left. \frac{\partial^2 W}{\partial y^2} + \frac{\partial^2 W}{\partial z^2} - \frac{Wc^2}{(1+cz)^2} + \frac{c}{1+cz} \frac{\partial W}{\partial z} - \frac{2c}{(1+cz)^2} \frac{\partial U}{\partial x} \right] \end{aligned} \quad (6c)$$

$$\frac{1}{1+cz} \frac{\partial U}{\partial x} + \frac{\partial V}{\partial y} + \frac{\partial W}{\partial z} + \frac{Wc}{1+cz} = 0 \quad (6d)$$

In the general orthogonal coordinates, the expressions for the rate-of-strain components are

$$\begin{aligned}
 e_{xx} &= 2 \left( \frac{1}{h_1} \frac{\partial U}{\partial x} + \frac{V}{h_1 h_2} \frac{\partial h_1}{\partial y} + \frac{W}{h_3 h_1} \frac{\partial h_1}{\partial z} \right) & e_{yz} &= \frac{h_3}{h_2} \frac{\partial}{\partial y} \left( \frac{W}{h_3} \right) + \frac{h_2}{h_3} \frac{\partial}{\partial z} \left( \frac{V}{h_2} \right) \\
 e_{yy} &= 2 \left( \frac{1}{h_2} \frac{\partial V}{\partial y} + \frac{W}{h_2 h_3} \frac{\partial h_2}{\partial z} + \frac{U}{h_1 h_2} \frac{\partial h_2}{\partial x} \right) & e_{zx} &= \frac{h_1}{h_3} \frac{\partial}{\partial z} \left( \frac{U}{h_1} \right) + \frac{h_3}{h_1} \frac{\partial}{\partial x} \left( \frac{W}{h_3} \right) \\
 e_{zz} &= 2 \left( \frac{1}{h_3} \frac{\partial W}{\partial z} + \frac{U}{h_3 h_1} \frac{\partial h_3}{\partial x} + \frac{V}{h_2 h_3} \frac{\partial h_3}{\partial y} \right) & e_{xy} &= \frac{h_2}{h_1} \frac{\partial}{\partial x} \left( \frac{V}{h_2} \right) + \frac{h_1}{h_2} \frac{\partial}{\partial y} \left( \frac{U}{h_1} \right)
 \end{aligned}$$

The viscous terms in equations (6a), (6b), and (6c) may be expressed using the rate-of-strain components as

$$\begin{aligned}
 \nu \left[ \frac{1}{(1+cz)^2} \frac{\partial^2 U}{\partial x^2} - \frac{z}{(1+cz)^3} \frac{\partial U}{\partial x} \frac{dc}{dx} + \frac{\partial^2 U}{\partial y^2} + \frac{\partial^2 U}{\partial z^2} + \frac{c}{1+cz} \frac{\partial U}{\partial z} - \frac{Uc^2}{(1+cz)^2} + \right. \\
 \left. \frac{W}{(1+cz)^3} \frac{dc}{dx} + \frac{2c}{(1+cz)^2} \frac{\partial W}{\partial x} \right] = \nu \left[ \frac{1}{1+cz} \frac{\partial e_{xx}}{\partial x} + \frac{\partial e_{yx}}{\partial y} + \frac{\partial e_{zx}}{\partial z} + \frac{2ce_{xz}}{1+cz} \right] \quad (7a)
 \end{aligned}$$

$$\begin{aligned}
 \nu \left[ \frac{1}{(1+cz)^2} \frac{\partial^2 V}{\partial x^2} - \frac{z}{(1+cz)^3} \frac{\partial V}{\partial x} \frac{dc}{dx} + \frac{\partial^2 V}{\partial y^2} + \frac{\partial^2 V}{\partial z^2} + \frac{c}{1+cz} \frac{\partial V}{\partial z} \right] = \\
 = \nu \left[ \frac{\partial e_{yy}}{\partial y} + \frac{1}{1+cz} \frac{\partial e_{xy}}{\partial x} + \frac{\partial e_{yz}}{\partial z} + \frac{c}{1+cz} e_{zy} \right] \quad (7b)
 \end{aligned}$$

$$\begin{aligned}
 \nu \left[ \frac{1}{(1+cz)^2} \frac{\partial^2 W}{\partial x^2} - \frac{U}{(1+cz)^3} \frac{dc}{dx} - \frac{z}{(1+cz)^3} \frac{\partial W}{\partial x} \frac{dc}{dx} + \frac{\partial^2 W}{\partial y^2} + \frac{\partial^2 W}{\partial z^2} - \frac{Wc^2}{(1+cz)^2} + \right. \\
 \left. \frac{c}{1+cz} \frac{\partial W}{\partial z} - \frac{2c}{(1+cz)^2} \frac{\partial U}{\partial x} \right] = \nu \left[ \frac{1}{1+cz} \frac{\partial e_{xz}}{\partial x} + \frac{\partial e_{yz}}{\partial y} + \frac{\partial e_{zz}}{\partial z} - \frac{c}{1+cz} (e_{xx} - e_{zz}) \right] \quad (7c)
 \end{aligned}$$

Equations (6) are directly applicable to the laminar flow. For turbulent flow, because of the velocity fluctuations it is necessary to modify the stresses by addition of the so-called Reynold's stresses. Thus, making use of the parallel form in equations (7), the Navier-Stokes equations of motion for turbulent flow may be written in terms of the apparent stresses as

$$\begin{aligned} & \frac{U}{1+cz} \frac{\partial U}{\partial x} + v \frac{\partial U}{\partial y} + w \frac{\partial U}{\partial z} + \frac{c}{1+cz} UW - \frac{1}{1+cz} \omega^2 R \frac{\partial R}{\partial x} + 2(\omega_y W - \omega_z V) \\ &= - \frac{1}{1+cz} \frac{1}{\rho} \frac{\partial P}{\partial x} + \frac{1}{\rho} \left[ \frac{1}{1+cz} \frac{\partial \sigma_x}{\partial x} + \frac{\partial \tau_{yx}}{\partial y} + \frac{\partial \tau_{zx}}{\partial z} + \frac{2c \tau_{zx}}{1+cz} \right] \end{aligned} \quad (8a)$$

$$\begin{aligned} & U \frac{\partial V}{\partial x} + v \frac{\partial V}{\partial y} + w \frac{\partial V}{\partial z} - \frac{1}{1+cz} \omega^2 R \frac{\partial R}{\partial y} + 2(\omega_z U - \omega_x W) \\ &= - \frac{1}{\rho} \frac{\partial P}{\partial y} + \frac{1}{\rho} \left[ \frac{1}{1+cz} \frac{\partial \tau_{xy}}{\partial x} + \frac{\partial \sigma_y}{\partial y} + \frac{\partial \tau_{yz}}{\partial z} + \frac{c \tau_{yz}}{1+cz} \right] \end{aligned} \quad (8b)$$

$$\begin{aligned} & \frac{U}{1+cz} \frac{\partial W}{\partial x} + v \frac{\partial W}{\partial y} + w \frac{\partial W}{\partial z} - \frac{c}{1+cz} U^2 - \omega^2 R \frac{\partial R}{\partial z} + 2(\omega_x V - \omega_y U) \\ &= - \frac{1}{\rho} \frac{\partial P}{\partial z} + \frac{1}{\rho} \left[ \frac{1}{1+cz} \frac{\partial \tau_{xz}}{\partial x} + \frac{\partial \tau_{yz}}{\partial y} + \frac{\partial \sigma_z}{\partial z} - \frac{c}{1+cz} (\sigma_x - \sigma_z) \right] \end{aligned} \quad (8c)$$

Simplification for flow within boundary layer. - Equations (6) and (8) are equivalent to the complete Navier-Stokes equations. Within the boundary layer, however, certain terms, whose contribution is relatively unimportant can be neglected. If the y-axis is taken as normal to the wall, the boundary-layer flow then takes place over the xz-plane (or the XZ-plane). All terms are now made dimensionless by referring the lengths to some body length, the velocities to their free-stream values, and so forth, as explained in reference 16 (p. 45) and all quantities of the order of magnitude of  $\delta$  or smaller are neglected. Furthermore, because the boundary-layer flow along a definite path  $z = 0$  is of interest, additional simplifications are possible. Setting  $z = 0$  restricts the equations, because the general boundary conditions (not on the x-axis) cannot be satisfied. It will subsequently be seen, however, that these general boundary conditions are unnecessary in the solution of the final equations. These simplifications yield the Navier-Stokes equations for flow within the boundary layer in a rotating orthogonal curvilinear coordinate system evaluated at  $z = 0$ ,

$$u \frac{\partial u}{\partial x} + v \frac{\partial u}{\partial y} + w \frac{\partial u}{\partial z} + cuw = - \frac{1}{\rho} \frac{\partial P}{\partial x} + \omega^2 R \frac{\partial R}{\partial x} - 2\omega_y w + v \left( \frac{\partial^2 u}{\partial y^2} \right) \quad (9a)$$

$$- \omega^2 R \frac{\partial R}{\partial y} + 2(\omega_z u - \omega_x w) = - \frac{1}{\rho} \frac{\partial P}{\partial y} \quad (9b)$$

$$u \frac{\partial w}{\partial x} + v \frac{\partial w}{\partial y} + w \frac{\partial w}{\partial z} - u^2 c = - \frac{1}{\rho} \frac{\partial P}{\partial z} + \omega^2 R \frac{\partial R}{\partial z} + 2\omega_y u + v \left( \frac{\partial^2 w}{\partial y^2} \right) \quad (9c)$$

for the laminar case. For the turbulent boundary layer, a corresponding set of equations is obtained with the substitution of  $\frac{1}{\rho} \frac{\partial \tau_{xy}}{\partial y}$  for  $v \left( \frac{\partial^2 u}{\partial y^2} \right)$  and  $\frac{1}{\rho} \frac{\partial \tau_{zy}}{\partial y}$  for  $v \left( \frac{\partial^2 w}{\partial y^2} \right)$ .

Equation (9b) shows, as pointed out in reference 10, that because all the terms on the left-hand side of the equations are of the order of magnitude of one, within the boundary layer,  $P$  can vary at most by an amount of the order of  $\delta$ . It is reasonable then to neglect this variation and consider  $P$  solely a function of the flow outside the boundary layer. Thus, if  $x$  is chosen to coincide with a streamline of the flow outside the boundary layer,  $V = W = 0$ , and by integration of equation (9a) with the effect of viscosity neglected the following relation is obtained:

$$P = \text{constant} - \frac{1}{2} \rho U^2 + \frac{1}{2} \rho \omega^2 R^2 \quad (10)$$

which is a form of the equation of Bernoulli.

Furthermore, because outside the boundary layer the flow with respect to some nonrotating set of coordinates is irrotational, with reference to the rotating coordinates the components of the vorticity vector become

$$\left. \begin{aligned} \xi &= -2\omega_x \\ \eta &= -2\omega_y \\ \zeta &= -2\omega_z \end{aligned} \right\} \quad (11)$$

This assumption of irrotationality is not always true and in some applications, such as the later stages of an axial compressor, it cannot be used. As long as vorticity is distributed according to some definite pattern, however, a relation between the components of vorticity and the components of rotational velocity may be found and substituted for equations (11).

Substituting again in the expression for the components of vorticity gives

$$-2\omega_y = \frac{1}{1+cz} \left[ \frac{\partial}{\partial z} (1+cz) U - \frac{\partial}{\partial x} W \right]$$



And for  $z = 0$ ,  $W = 0$ , which is along the streamline, the expression for curvature becomes

$$c = - \left( \frac{2\omega_y}{U} + \frac{1}{U} \frac{\partial U}{\partial z} \right) \quad (12)$$

The equation of continuity remains

$$\frac{\partial u}{\partial x} + \frac{\partial v}{\partial y} + \frac{\partial w}{\partial z} + wc = 0 \quad (13)$$

Generalized boundary-layer momentum-integral equations. - In order to obtain the boundary-layer momentum-integral equations, equations (9a) and (9c) are integrated with respect to  $y$  through the boundary layer to some constant height  $d$  such that

$$\begin{aligned} & d \geq \delta \\ & \frac{\partial}{\partial x} \int_0^d u^2 dy + 2\omega_y \int_0^d w dy + \frac{\partial U}{\partial z} \int_0^d w dy - U \frac{\partial}{\partial x} \int_0^d u dy - U \frac{\partial}{\partial z} \int_0^d w dy + \\ & \frac{\partial}{\partial z} \int_0^d uw dy - 4 \frac{\omega_y}{U} \int_0^d uw dy - 2 \frac{1}{U} \frac{\partial U}{\partial z} \int_0^d uw dy + 2\omega_y \int_0^d w dy = U d \frac{\partial U}{\partial x} - \frac{\tau_{0,x}}{\rho} \end{aligned} \quad (14a)$$

and

$$\begin{aligned} & \frac{\partial}{\partial x} \int_0^d uw dy + \frac{\partial}{\partial z} \int_0^d w^2 dy + c \int_0^d w^2 dy - c \int_0^d u^2 dy \\ & = U \frac{\partial U}{\partial z} \int_0^d dy + 2\omega_y \int_0^d u dy - \frac{\tau_{0,z}}{\rho} \end{aligned} \quad (14c)$$

These equations apply equally well for the laminar or turbulent boundary layer, with the value of  $\tau_0$  representing the shear stress at the wall accordingly adjusted. By suitable use of equations (12) and (13), these equations may be transformed to

$$\begin{aligned} & \frac{\partial}{\partial x} \int_0^d (U-u)u \, dy + \frac{\partial U}{\partial x} \int_0^d (U-u) \, dy + \frac{\partial}{\partial z} \int_0^d (U-u)w \, dy - \\ & \frac{2}{U} \frac{\partial U}{\partial z} \int_0^d (U-u)w \, dy - \frac{4\omega y}{U} \int_0^d (U-u)w \, dy = \frac{\tau_{0,x}}{\rho} \end{aligned} \quad (15a)$$

and

$$\begin{aligned} & \frac{\partial}{\partial x} \int_0^d uw \, dy + \frac{\partial}{\partial z} \int_0^d w^2 \, dy - \frac{1}{U} \frac{\partial U}{\partial z} \int_0^d w^2 \, dy + \frac{1}{U} \frac{\partial U}{\partial z} \int_0^d u^2 \, dy \\ & = U \frac{\partial U}{\partial z} \int_0^d dy + 2\omega y \int_0^d u \, dy + \frac{2\omega y}{U} \int_0^d w^2 \, dy - \frac{2\omega y}{U} \int_0^d u^2 \, dy - \frac{\tau_{0,z}}{\rho} \end{aligned} \quad (15c)$$

The following definitions are now introduced: The momentum thickness in the x-direction of the flow in the x-direction,

$$\theta_x = \frac{1}{U^2} \int_0^d (U-u)u \, dy \quad (16)$$

The displacement thickness in the x-direction,

$$\delta_x^* = \frac{1}{U} \int_0^d (U-u) \, dy \quad (17)$$

The momentum thickness in the z-direction of the flow in the z-direction,

$$\theta_z = \frac{1}{U^2} \int_0^d w^2 \, dy \quad (18)$$

The displacement thickness in the z-direction,

$$\delta_z^* = \frac{1}{U} \int_0^d w \, dy \quad (19)$$

The momentum thickness in the z-direction of the flow in the x-direction,

$$\theta_{xz} = \frac{1}{U^2} \int_0^d (U-u)w \, dy \quad (20)$$

The momentum thickness in the x-direction of the flow in the z-direction,

$$\theta_{zx} = \frac{1}{U^2} \int_0^d wu \, dy \quad (21)$$

All these thicknesses, as in two-dimensional boundary-layer theory, have a dimension of length. Furthermore,

$$\delta_z^* - \theta_{xz} = \frac{1}{U} \int_0^d w \, dy - \frac{1}{U^2} \int_0^d (U-u)w \, dy = \frac{1}{U^2} \int_0^d uw \, dy = \theta_{zx} \quad (22)$$

With the use of definitions (16) to (21) and equation (22), equations (15a) and (15c) reduce for  $z = 0$ , to

$$\frac{\partial \theta_x}{\partial x} + \frac{1}{U} \frac{\partial U}{\partial x} (2\theta_x + \delta_x^*) + \frac{\partial \theta_{xz}}{\partial z} - 4 \frac{\omega_y}{U} \theta_{xz} = \frac{\tau_{0,x}}{\rho U^2} \quad (23a)$$

and

$$\frac{\partial \theta_z}{\partial z} + \frac{\partial (\delta_z^* - \theta_{xz})}{\partial x} + \frac{1}{U} \frac{\partial U}{\partial z} (\theta_z - \theta_x - \delta_x^*) + \frac{2}{U} \frac{\partial U}{\partial x} (\delta_z^* - \theta_{xz}) - \frac{2\omega_y}{U} (\theta_x + \theta_z) = - \frac{\tau_{0,z}}{\rho U^2} \quad (23c)$$

Reduction of equations to forms obtained by other investigators. - If only two-dimensional flow exists, that is if  $c = 0$ ,  $w = 0$ , and  $\omega = 0$ , then equation (23c) vanishes and equation (23a) becomes an ordinary Kármán momentum-integral equation

$$\frac{\partial \theta_x}{\partial x} + \frac{1}{U} \frac{\partial U}{\partial x} (2\theta_x + \delta_x^*) = \frac{\tau_{0,x}}{\rho U^2}$$

If  $\omega = 0$ , that is, if the system is nonrotating, equations (23a) and (23c) become identical with the equations of Gruschwitz (reference 9).

Setting  $c = 0$  in equations (9a) and (9c) makes these equations identical with the equations of Burgers (reference 10), who carried out his derivation for a Cartesian coordinate system.

Finally, if the system of coordinates is chosen so as to maintain the right-hand rule and  $c$  is set equal to  $\frac{1}{r}$ , thus establishing the  $x$ -axis as a circle, then  $\frac{dz}{dr} = 1$  and because of axial symmetry all derivatives with respect to  $x$  vanish. The coordinates are now assumed to be in a fluid that is motionless at great distance from the surface of the rotating immersed disk. Thus,

$$U = W = 0 \quad \omega = 0$$

Integration of equations (9a) and (9c) gives after some manipulation,

$$2\pi \frac{d}{dr} \left( r^2 \int_0^d uw \, dy \right) = - \frac{\tau_{0,x}}{\rho} 2\pi r^2$$

and

$$\frac{d}{dr} \left( r \int_0^d w^2 \, dy \right) - \int_0^d u^2 \, dy = - \frac{\tau_{0,z}}{\rho} r$$

which are identical with equations of von Kármán for the rotating disk (reference 17).

#### APPROXIMATE SOLUTION OF MOMENTUM-INTEGRAL EQUATIONS

##### FOR TURBULENT BOUNDARY LAYER

Transformation and reduction of dependent variables. - In order to obtain a solution of the momentum-integral equations, additional relations are needed describing the velocity profiles existing in the boundary layer and the friction at the wall.

With the use of a suggestion by Prandtl (reference 11), the expressions for  $u$  and  $w$  that will be used are

$$\left. \begin{aligned} u &= UG\left(\frac{y}{\delta}\right) \\ w &= \epsilon UG\left(\frac{y}{\delta}\right)g\left(\frac{y}{\delta}\right) = \epsilon ug \end{aligned} \right\} \quad (24)$$

with boundary conditions on  $G$  and  $g$

$$\text{for } y = \delta, \quad G = 1, \quad g = 0$$

$$\text{for } y = 0, \quad G = 0, \quad g = 1$$

and with  $\epsilon$  defined as

$$\epsilon \equiv \tan \alpha \quad (25)$$

where  $\alpha$  is the angle between the direction of the resultant skin-friction stress and the direction of the flow outside the boundary layer. Because of this definition of  $\epsilon$ ,  $g = 1$  at  $y = 0$  because

$$\lim_{y \rightarrow 0} \frac{\frac{\partial w}{\partial y}}{\frac{\partial u}{\partial y}} = \epsilon$$

or

$$\tau_{0,z} = \epsilon \tau_{0,x} \quad (26)$$

Mathematically, such use of  $\epsilon$  implies a linear variation of  $w$  with  $\epsilon$  and makes possible the dissociation of the  $w$  velocity profile from its scale and direction. Because the flow must change direction in the boundary layer from that at the wall to that in the free stream, there is no reason to assume that such a dissociation is actually possible. In other words, there is no reason to believe that  $g$  should be a function of  $(y/\delta)$  alone and not of  $\epsilon$  as well. In accordance with reference 11, however, this approximation is certainly admissible for small values of  $\epsilon$  and gives results of qualitative accuracy for moderately large  $\epsilon$ . In addition, in order to check this assumption, the value of  $\frac{1}{\epsilon} \frac{w}{U}$ , for several experimental velocity profiles and values of  $\epsilon$  ranging from 0.216 to 0.670, as obtained from reference 9, is plotted against  $y/\delta$  in figure 3. The results of this plot indicate indeed that  $Gg$  is independent of  $\epsilon$ .

In parallel to the two-dimensional boundary-layer theory, the following definitions are made:

$$\left. \begin{aligned} \frac{\int_0^d (1-G) dy}{\int_0^d (1-G)G dy} &\equiv H \\ \frac{\int_0^d (1-G)Gg dy}{\int_0^d (1-G)G dy} &\equiv J \\ \frac{\int_0^d Gg dy}{\int_0^d (1-G)G dy} &\equiv K \\ \frac{\int_0^d G^2g^2 dy}{\int_0^d (1-G)G dy} &\equiv L \end{aligned} \right\} \quad (27)$$

The relations among the various thicknesses may then be written

$$\left. \begin{aligned} \delta_x^* &= H\theta_x \\ \theta_{xz} &= \epsilon J\theta_x \\ \delta_z^* &= \epsilon K\theta_x \\ \theta_z &= \epsilon^2 L\theta_x \end{aligned} \right\} \quad (28)$$

The quantities  $H$ ,  $J$ ,  $K$ , and  $L$  are functions of  $G$  and  $g$ . Because  $G$  and  $g$  are representative of the velocity profiles in the boundary layer, the changes in these velocity profiles must be reflected in turn in the values of  $H$ ,  $K$ ,  $J$ , and  $L$ . In other words, the

external forces acting on the boundary layer and influencing the changes in the shape of the velocity profiles also cause a variation in  $H$ ,  $K$ ,  $J$ , and  $L$ . Unfortunately, the available data of reference 9, do not involve large changes in the shape of the velocity profiles and the quantities  $H$ ,  $J$ ,  $K$ , and  $L$ . This behavior of the velocity profiles is verified in figure 3. The data of reference 12 do indicate large changes in the shape of the velocity profile; however, the data are not presented with sufficient detail to permit an accurate evaluation of  $H$ ,  $J$ ,  $K$ , and  $L$ . Thus, until more extensive experimental data become available, the quantities  $H$ ,  $J$ ,  $K$ , and  $L$  are assumed to be constants that can be evaluated either by assuming a suitable form for  $G$  and  $g$  or by computing directly from Gruschwitz data.

In accordance with reference 9, good assumptions for  $G$  and  $g$  are:

$$\left. \begin{aligned} G &= \left(\frac{y}{\delta}\right)^{\frac{1}{n}} \\ g &= \left(1 - \frac{y}{\delta}\right)^2 \end{aligned} \right\} \quad (29)$$

An indication of the degree of fit afforded by these expressions can be obtained from figure 4(a), where a calculated profile with  $n = 7$  is compared with one of the profiles of Gruschwitz. Other profiles of Gruschwitz data give similar results. It should be noted that this good agreement should not be interpreted as meaning that assumptions (29) will always give a good representation of the velocity profiles in the three-dimensional turbulent boundary layer. Figure 4(b) shows a comparison similar to that of figure 4(a) with profiles converted to the  $x, y, z$  system using data from reference 12. Equations (29) do not afford a good fit in figure 4(b), although the equations do represent the general behavior of the velocities. This comparison is further illustrated in figure 5, where the value of  $g(y/\delta)$  as obtained by converting the profiles of reference 12 to the  $x, y, z$  system at indicated points is compared with  $(1 - y/\delta)^2$ .

With the use of relations (29),  $H$ ,  $K$ ,  $J$ , and  $L$  are computed as

$$\left. \begin{aligned}
 H &= \frac{2+n}{n} \\
 J &= \frac{n^2(11n+7)}{(2n+1)(3n+1)(3n+2)} \\
 K &= \frac{2n^2(2+n)}{(2n+1)(3n+1)} \\
 L &= \frac{6n^4}{(3n+2)(2n+1)(5n+2)}
 \end{aligned} \right\} \quad (30)$$

which for  $n = 7$  give

$$\left. \begin{aligned}
 H &= 1.2857 \\
 J &= 0.5423 \\
 K &= 2.6727 \\
 L &= 1.1285
 \end{aligned} \right\} \quad (30a)$$

Averaging the values along line III of Gruschwitz data (fig. 2) results in

$$\left. \begin{aligned}
 H &= 1.37 \\
 J &= 0.550 \\
 K &= 2.43 \\
 L &= 0.968
 \end{aligned} \right\} \quad (30b)$$

This relatively good agreement between the two sets of values is also indicative of the over-all fit of the assumed expressions for  $G$  and  $g$  to the data of reference 9.

The additional relation that is needed for the solution of the momentum-integral equation is the expression for surface friction. In reference 9, Gruschwitz demonstrates that von Kármán's friction law

$$\frac{\tau_{0,x}}{\rho U^2} = 0.01255 \left( \frac{v}{U \theta_x} \right)^{\frac{1}{4}} \quad (31)$$

appears to be valid in the three-dimensional boundary layer as well.



Substituting relations (26), (28), and (31) in equations (23) gives

$$\frac{\partial \theta_x}{\partial x} + \frac{\theta_x}{U} \frac{\partial U}{\partial x} (2+H) + J\epsilon \frac{\partial \theta_x}{\partial z} + J\theta_x \frac{\partial \epsilon}{\partial z} - 4 \frac{\omega_y}{U} J\epsilon \theta_x = \frac{\tau_{0,x}}{\rho U^2} \quad (32a)$$

and

$$\begin{aligned} 2L\theta_x \epsilon \frac{\partial \epsilon}{\partial z} + L\epsilon^2 \frac{\partial \theta_x}{\partial z} + (K-J)\theta_x \frac{\partial \epsilon}{\partial x} + (K-J)\epsilon \frac{\partial \theta_x}{\partial x} + (L\epsilon^2 - 1 - H) \frac{\theta_x}{U} \frac{\partial U}{\partial z} + \\ 2(K-J)\epsilon \frac{\theta_x}{U} \frac{\partial U}{\partial x} - (1+L\epsilon^2) \frac{2\omega_y}{U} \theta_x = -\epsilon \frac{\tau_{0,x}}{\rho U^2} \end{aligned} \quad (32c)$$

Because of the form of the relation for friction, an advantageous transformation of variable is

$$\Theta = \theta_x R^{\frac{1}{4}}(\theta_x) \quad (33)$$

in order to "remove" the Reynolds number from the equations.

With the use of equations (33) and (12), two nonlinear partial differential equations for  $\Theta$  and  $\epsilon$  applying along  $z = 0$  are obtained from equations (32),

$$\frac{4}{5} \frac{\partial \Theta}{\partial x} + \frac{4}{5} J\epsilon \frac{\partial \Theta}{\partial z} + J\Theta \frac{\partial \epsilon}{\partial z} + \left\{ \left[ \left( \frac{5H+9}{5} \right) \frac{1}{U} \frac{\partial U}{\partial x} + \frac{J}{5} c\epsilon - \frac{18}{5} J\epsilon \frac{\omega_y}{U} \right] \Theta - 0.01255 \right\} = 0 \quad (34a)$$

and

$$\begin{aligned} \frac{4}{5} (K-J)\epsilon \frac{\partial \Theta}{\partial x} + \frac{4}{5} L\epsilon^2 \frac{\partial \Theta}{\partial z} + (K-J)\Theta \frac{\partial \epsilon}{\partial x} + 2L\Theta\epsilon \frac{\partial \epsilon}{\partial z} + \\ \left[ \frac{9}{5} (K-J)\epsilon \frac{\Theta}{U} \frac{\partial U}{\partial x} - \left( \frac{4}{5} L\epsilon^2 - 1 - H \right) c\Theta - \left( \frac{9L}{5} \epsilon^2 - H \right) \frac{2\omega_y}{U} \Theta + 0.01255\epsilon \right] = 0 \end{aligned} \quad (34c)$$

As shown in the appendix, these equations can be either hyperbolic, parabolic, or elliptic, depending on the shape of the velocity profiles existing in the boundary layer. For  $u = U(y/\delta)^{1/n}$  and  $g = (1-y/\delta)^2$ , the equations are always elliptic.

Simplification of equations and approximate solution. - The relative importance of the various derivatives in equations (34) is now determined. First,  $\Theta$  and  $\epsilon$  are assumed to be quantities that are smaller than one, which can be accomplished simply by referring all lengths to a total path length  $S$  and  $\alpha$  to  $45^\circ$ . As a result of this assumption, all derivatives in  $\Theta$  and  $\epsilon$  become of the order of magnitude of  $\Theta$  or  $\epsilon$ . Equation (34a) is then divided by  $4/5$ , so that the coefficient of  $\partial\Theta/\partial x$  is 1 and the coefficients of  $\partial\Theta/\partial z$  and  $\partial\epsilon/\partial z$  are  $J\epsilon$  and  $\frac{5}{4}J\Theta$  that is, of the order of magnitude of  $\epsilon$  or  $\Theta$ , respectively. In a similar way equation (34c) is divided by  $(K-J)\Theta$  so that the coefficients of  $\partial\Theta/\partial x$  and  $\partial\epsilon/\partial x$  become  $\frac{4}{5}\epsilon/\Theta$  and 1 (order of magnitude of one), respectively, and those of  $\partial\Theta/\partial z$  and  $\partial\epsilon/\partial z$  become  $\frac{4}{5}L\frac{\epsilon}{\Theta}$  and  $2L\epsilon$  (order of magnitude of  $\epsilon$ ), respectively. Then, if  $\epsilon$  is small as compared with  $\tan 45^\circ$  and  $\Theta$  is small when compared with  $S$ , all terms of the order of magnitude of  $\epsilon^2$ ,  $\Theta\epsilon$ , or  $\Theta^2$  may be neglected, which gives

$$\frac{\partial\Theta}{\partial x} + \left[ \left( \frac{5H+9}{4} \right) \frac{1}{U} \frac{\partial U}{\partial x} \right] \Theta = 0.01569 \quad (35a)$$

and

$$\frac{\partial\epsilon}{\partial x} + \left[ \frac{4}{5} \frac{1}{\Theta} \frac{\partial\Theta}{\partial x} + \frac{9}{5} \frac{1}{U} \frac{\partial U}{\partial x} + \frac{0.01255}{(K-J)} \frac{1}{\Theta} \right] \epsilon = \frac{1}{(J-K)} \left[ (1+H)c + H \frac{2\omega_y}{U} \right] \quad (35c)$$

These two expressions show that the primary changes in  $\Theta$  and  $\epsilon$  in equations (34a) and (34c) occur only in the  $x$ -direction and thus the description of the phenomena only at  $z = 0$  is justified.

A solution of equations (35) can now be obtained by successive approximations because  $U$ ,  $\omega_y$ , and  $c$  are assumed to be known functions of  $x$ . First, equation (35a) is solved,

$$\Theta_I = \Theta_i \left( \frac{U_i}{U} \right)^{\left( \frac{5H+9}{4} \right)} + \frac{0.01569}{\left( \frac{5H+9}{4} \right)} \int_{x_i}^x U^{\left( \frac{5H+9}{4} \right)} dx \quad (36)$$

The values of  $\Theta_I(x)$  are then used in an approximate solution of equation (35c)

$$\epsilon_I = \epsilon_i \left( \frac{\Theta_i}{\Theta_I} \right)^{\frac{4}{5}} \left( \frac{U_i}{U} \right)^{\frac{9}{5}} \frac{1}{E_1(x)} + \frac{1}{(J-K)(\Theta_I)^{\frac{4}{5}} U^{\frac{9}{5}} E_1(x)} \int_{x_1}^x \left[ (1+H)c + H \frac{2\omega_y}{U} \right] \left( \frac{\Theta}{\Theta_I} \right)^{\frac{4}{5}} U^{\frac{9}{5}} E_1(x) dx \quad (37)$$

where

$$E_1(x) \equiv e^{\frac{0.01255}{(K-J)} \int_{x_1}^x \frac{dx}{\Theta_I}} \quad (38)$$

With  $\epsilon_I(x)$  known, the approximation for  $\Theta$  could in turn, be improved by again solving equation (35a). If  $\alpha$  grows large along the path, however, it is more advantageous to consider the following equation:

$$\frac{\partial \Theta}{\partial x} + J\epsilon \frac{\partial \Theta}{\partial z} + \left[ \left( \frac{5H+9}{4} \right) \frac{1}{U} \frac{\partial U}{\partial x} + \frac{J}{4} c\epsilon - \frac{18}{4} J\epsilon \frac{\omega_y}{U} \right] \Theta = 0.01569 \quad (39)$$

It is thus hoped that neglect of  $\partial \epsilon / \partial z$  will not affect the accuracy of the solution to a very marked extent. The solution of equation (39), which may be obtained by the method of Lagrange, is

$$\Theta_{II} = \left[ \psi \left( z - J \int_{x_1}^x \epsilon dx \right) \right] \frac{E_3(x)}{U \left( \frac{5H+9}{4} \right) E_2(x)} + \frac{0.01569 E_3(x)}{U \left( \frac{5H+9}{4} \right) E_2(x)} \int_{x_1}^x \frac{U \left( \frac{5H+9}{4} \right) E_2(x)}{E_3(x)} dx \quad (40)$$

where

$$E_2(x) \equiv e^{\frac{J}{4} \int_{x_1}^x c\epsilon dx} \quad (41)$$

$$E_3(x) \equiv e^{\frac{18}{4} J \int_{x_1}^x \epsilon \frac{\omega_y}{U} dx} \quad (42)$$

and

$$\psi \left( z - J \int_{x_1}^x \epsilon \, dx \right)$$

is an arbitrary function satisfying the boundary condition; when  $x = x_1$  and  $z = 0$ , then  $\Theta_{II} = \Theta_1$ . Setting

$$\left( z - J \int_{x_1}^x \epsilon \, dx \right) = \lambda$$

at  $x = x_1$  gives  $\lambda = 0$ . In addition, for  $z = 0$ ,  $\lambda$  is of the order of magnitude of  $\epsilon$ .

Expansion of  $\psi$  in Maclaurin's series about  $\lambda(x_1)$  yields

$$\psi(\lambda) = \psi(0) + \lambda \psi'(0) + \frac{\lambda^2}{2!} \psi''(0) + \dots$$

Because there is only one boundary condition, it is possible to determine only one of the constants in this expansion; consequently,  $\psi$  cannot be uniquely established. The fact that  $\lambda$  is of the order of magnitude of  $\epsilon$ , however, suggests that the assumptions made for  $\psi''(0)$ ,  $\psi'''(0)$ , and so forth, are successively less important. Thus these derivatives may arbitrarily be expressed by a single constant,

$$\psi(\lambda) = \Theta_1 U_1 \left( \frac{5H+9}{4} \right) \left( 1 + A\lambda + \frac{A^2 \lambda^2}{2!} + \dots \right) = \Theta_1 U_1 \left( \frac{5H+9}{4} \right) e^{A\lambda} \quad (43)$$

where  $A$  from purely dimensional considerations must have the dimensions of  $\lambda^{-1}$ . From expressions (41) and (42), it is suspected that

$$A = B \left( \frac{c}{4} - \frac{18}{4} \frac{\omega y}{U} \right)_1 \quad (44)$$

where  $B$  must be obtained from the experimental measurements.

It should be noted that because  $\psi(\lambda)$  cannot be uniquely determined other functions of  $\lambda$  satisfying the single boundary condition could be used as well. The function  $e^{A\lambda}$  is chosen only because it is convenient to use and parallels the expressions (41) and (42). This arbitrariness of the functional form of  $\psi$  and the value of  $A$  is due to the consequences of assuming  $z = 0$ , and thus it is probably not advisable to carry any further approximation for  $\epsilon_{II}$ , and so forth.

In solving equations (36) to (44), either set of values for  $H$ ,  $K$ ,  $J$ , and  $L$  may be used. Because the averaged values (30b) are probably more representative, having been obtained by evaluating experimental data at a number of different positions, it is advantageous to use these values in computations.

#### COMPARISON WITH EXPERIMENT

In order to check the validity of the approximate solution, the boundary layer along four streamlines of reference 9 was computed and compared with the measured values. The designation of the streamlines and data points is illustrated in figure 2. Because the data were taken along curves I to V of figure 2, the computation along a streamline requires first an interpolation among the various data points. As a result of this interpolation, the computations could not be carried through the full length of each streamline. Values (30b) were used for quantities  $H$ ,  $K$ ,  $J$ , and  $L$ . The constant  $B$  was obtained by fitting along streamline "B" the solution for  $\Theta_{II}$ , so that at  $x = S$ ,  $\Theta_{II} \sim \Theta$  measured. In this manner, the value of  $B$  was found to be 38.5. This value was then used in computations of streamlines "A", "C", and "D". It is noted that  $B = 38.5 \sim 7R^{1/4}(\theta_x)_1$ , although justification for such a dependence cannot be made. In all integrations Simpson's rule was used.

The results of the computations are plotted in a nondimensional form and compared with interpolated measured values in figures 6 and 7. A study of these figures reveals a fair quantitative agreement between the measured and estimated values of  $\Theta$  and  $\alpha$ . As the values of  $\epsilon \rightarrow \tan 45^\circ$  (fig. 7) the first approximation for  $\Theta$  in figure 6 becomes progressively worse, which is remedied by the second approximation. The poorest agreement is obtained along streamlines "A" and "D", which because they are closest to the walls might be affected by the flow in the corners of the duct. Streamline "D" especially may thus be affected inasmuch as Gruschwitz mentions the existence of separation on the convex wall.

The fair quantitative agreement with the measured values is not to be interpreted as a conclusive check of the validity of the procedure and the assumed values in all cases of three-dimensional boundary-layer flow. The suggested procedure simply represents the best that can be done in view of the meagerness of the available data. Because the Gruschwitz data do not involve the effects of uniform angular velocity and because the variations in  $\frac{1}{U} \frac{\partial U}{\partial x}$  and  $\frac{1}{U} \frac{\partial U}{\partial z}$  are small, it could be maintained that this check of the procedure has been carried out

on a somewhat special case. For that reason, it is desirable that additional experiments be carried out in setups that eliminate the present shortcomings. Larger variation of Reynolds number should also be used. With additional experiments, a modification of the values of  $H$ ,  $K$ ,  $J$ ,  $L$ , and  $B$ , together perhaps with some refinements of the procedure will be in order. It might be well to remember at such time, that because of the necessary empiricism involved (which results from the very limited knowledge of turbulent phenomena), long and tedious computations would rarely be worthwhile.

### CONCLUSIONS

The following conclusions can be drawn from an analysis of the three-dimensional momentum-integral equations and a comparison of the numerical results with the Gruschwitz data for turbulent boundary layer:

1. Within the boundary layer the static pressure can vary at most by an amount of the order of magnitude of the boundary-layer thickness  $\delta$ .
2. It is possible to generalize the velocities in the boundary layer by use of two characteristic quantities  $\delta$  and  $\epsilon$  where  $\epsilon$  is the tangent of the angle enclosed by the direction of the resultant skin-friction stress and the direction of the flow outside the boundary layer.
3. When the generalized boundary-layer momentum-loss thickness  $\Theta$  is small as compared with the total path length and  $\epsilon$  is small as compared with  $\tan 45^\circ$ , the primary changes in  $\Theta$  and  $\epsilon$  occur along the streamline of the flow outside the boundary layer.
4. The three-dimensional boundary-layer momentum-integral equations can be either hyperbolic, parabolic, or elliptic, depending on the relative magnitude of the parameter  $MN$ , which in turn depends on the shape of the velocity profiles existing in the boundary layer. The power-law profile when used with the correction function  $g = (1-y/\delta)^2$  always results in elliptic equations.
5. The approximate solution of the three-dimensional momentum-integral equations shows a fair quantitative agreement with the values measured by Gruschwitz.
6. Additional experimental data are necessary to establish more generally applicable values for form parameters  $H$ ,  $K$ ,  $J$ , and  $L$  and  $B$ , the constant used in the second approximation for  $\Theta$ .

Lewis Flight Propulsion Laboratory,  
National Advisory Committee for Aeronautics,  
Cleveland, Ohio, November 1, 1950.

# APPENDIX - ADDITIONAL REMARKS ON THREE-DIMENSIONAL BOUNDARY-LAYER MOMENTUM-INTEGRAL EQUATIONS

In order to obtain the approximate solution of equation (34), it was shown by comparing the relative order of magnitude of the coefficients that some of the terms may be neglected. Care must be taken with such simplifications inasmuch as various implications of the equations in question may be obscured by this procedure. For this reason, aside from the approximate solution, the character of equations (34) was also investigated in detail.

By use of the procedure outlined in reference 18 (p. 38), along  $z = 0$  the system of equations (34) is found to be hyperbolic when  $MN > 1$ , elliptic when  $MN < 1$ , and parabolic when  $MN = 1$ .

where

$$MN \equiv \frac{L}{(K-J)J} = \frac{\theta_x \theta_z}{\theta_{xz} \theta_{zx}} \neq 0 \quad (45)$$

Because  $L$ ,  $K$ , and  $J$  are functions of  $G$  and  $g$ , the character of equation (34) depends on the shape of the velocity profiles in the boundary layer.

It should be noted that when  $MN = 0$ , then  $L = 0$ , which is only possible if  $G = 0$  or  $g = 0$ , and in turn  $u = 0$  or  $w = 0$ . If the trivial case  $u = 0$  is neglected, it is established that when  $w = 0$ ,  $\epsilon = 0$  as well. But for  $\epsilon = 0$  and  $w = 0$ , equations (34) reduce to a special case

$$\frac{4}{5} \frac{\partial \Theta}{\partial x} + \frac{\Theta}{U} \frac{\partial U}{\partial x} \left( \frac{5H+9}{5} \right) = 0.01255 \quad (46a)$$

and

$$\frac{2\omega_y}{U} - \frac{1+H}{H} \cdot c = - \frac{0.01255}{\Theta} \quad (46c)$$

Here equation (46a) is an ordinary two-dimensional boundary-layer momentum-integral equation for  $\Theta$  and equation (46c) is a relation that evidently must exist among  $U$ ,  $\partial U / \partial z$ ,  $\omega_y$ , and  $\Theta$ , when  $\epsilon = 0$  and  $w = 0$ .

When the equations are elliptic, no real characteristic direction can be found. When only one characteristic direction exists, the equations are parabolic and in the hyperbolic case two characteristic directions through each point of the  $xz$ -plane are obtained. For the parabolic case then,

$$\frac{dz}{dx} = \zeta_p = J\epsilon$$

and for the hyperbolic case,

$$\frac{dz}{dx} = \zeta_+ = \epsilon \frac{L + \sqrt{L^2 - J(K-J)L}}{(K-J)}$$

$$\frac{dz}{dx} = \zeta_- = \epsilon \frac{L - \sqrt{L^2 - J(K-J)L}}{(K-J)}$$

and the characteristic lines are asymmetric with respect to the  $x$ -axis. In order to determine whether elliptic, parabolic, or hyperbolic equations apply, the magnitude of  $MN$  is computed. Substituting from expressions (30),  $MN$  is obtained in terms of  $n$ :

$$MN = \frac{6(3n+1)(3n+2)}{(5n+2)(11n+7)} = 1 - \frac{1}{55} - \frac{108n+96}{55(55n^2+57n+14)}$$

This equation shows  $MN$  to be a monotonically increasing function of  $n$ . For  $n = 0$ ,

$$MN = \frac{6}{7}$$

and

$$\lim_{n \rightarrow \infty} MN = \frac{54}{55}$$

These results indicate that a so-called power-law profile when used with  $g = (1-y/\delta)^2$  always results in equations that although elliptic are very near to being parabolic. Using values (30b),

$$MN = 0.936$$

which again indicates an elliptic character of the equations. It should be remembered, however, that the assumption for  $G$  and  $g$  were made on the basis of only one set of data; consequently there is no assurance



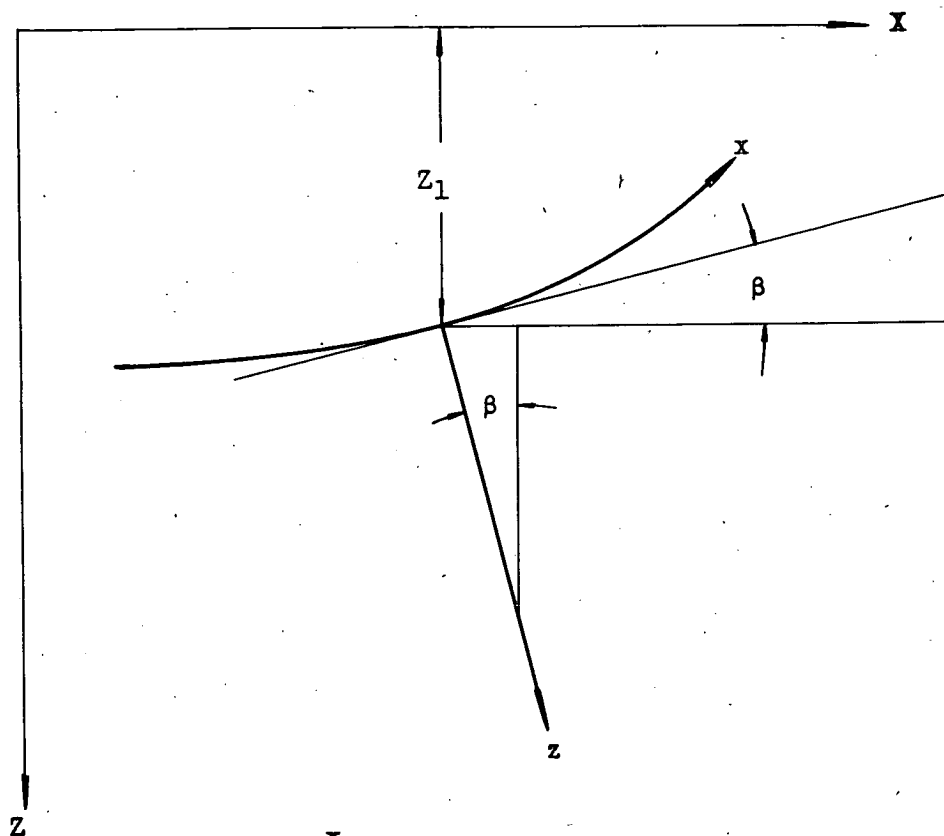
that the velocity distributions existing in the boundary layer will always give the same values of  $MN$ . In fact, it is generally more likely that they will not give the same values of  $MN$ . Some indication of the variation of  $MN$  may already be obtained from figure 8, where its value was plotted for each Gruschwitz data point. At points 5, 6, and 7, however, small values of  $w$  may have prevented an accurate determination of  $L$  and as a consequence  $MN = 0$  there. The value of  $MN$  in figure 8, varies within the limits  $0.65 < MN < 1.2$ , with the bulk of the points indicating that  $MN \sim 0.95$ .

On the basis of the preceding discussion, there is some evidence of the equations being parabolic, elliptic, and hyperbolic in the turbulent boundary layer. It is interesting to note that generally (as in supersonic and subsonic flow, for instance), these hyperbolic and elliptic regions have their counterpart in physical phenomena. Thus some essential differences might exist in the process of momentum transfer between the hyperbolic and elliptic regions. These differences cannot now be ascertained because first equations similar to (34) with  $z \neq 0$  would have to be obtained, and there is no mention of any irregularities in the behavior of the flow in reference 9. When additional experiments are made, however, it would seem advisable to closely study these two mathematical regions in order to obtain some indication of the physical make-up of their differences.

#### REFERENCES

1. Weske, John R.: An Investigation of the Aerodynamic Characteristics of a Rotating Axial-Flow Blade Grid. NACA TN 1128, 1947.
2. Ruden, P.: Investigation of Single Stage Axial Fans. NACA TM 1062, 1944.
3. Weske, John R.: Fluid Dynamic Aspects of Axial-Flow Compressors and Turbines. Jour. Aero. Sci., vol. 14, no. 11, Nov. 1947, pp. 651-656.
4. Weske, J. R.: Secondary Flows in Rotating Blade Passages at High Reynolds Numbers. Proc. Seventh Int. Cong. for Appl. Mech., vol. 2, pt. 1, 1948, pp. 155-163.
5. Jones, Robert T.: Effects of Sweepback on Boundary-Layer and Separation. NACA Rep. 884, 1947. (Formerly NACA TN 1402.)
6. Sears, W. R.: The Boundary Layer of Yawed Cylinders. Jour. Aero. Sci., vol. 15, no. 1, Jan. 1948, pp. 49-52.

7. Wild, J. M.: The Boundary Layer of Yawed Infinite Wings. Jour. Aero. Sci., vol. 16, no. 1, Jan. 1949, pp. 41-45.
8. Tetervin, Neal: Boundary-Layer Momentum Equations for Three-Dimensional Flow. NACA TN 1479, 1947.
9. Gruschwitz, E.: Turbulente Reibungsschichten mit Sekundärströmung. Ingenieur-Archiv, Bd. VI, 1935, S. 355-365.
10. Burgers, J. M.: Some Considerations on the Development of Boundary Layers in the Case of Flows Having a Rotational Component. Nederl. Akad. van Wetenschappen, vol. XLIV, Nos. 1-5, 1941, pp. 12-25.
11. Prandtl, L.: On Boundary Layers in Three-Dimensional Flow. Reps. and Trans. No. 64, British M.A.P., May 1, 1946.
12. Kuethe, A. M., McKee, P. B., and Curry, W. H.: Measurements in the Boundary Layer of a Yawed Wing. NACA TN 1946, 1949.
13. Lamb, Horace: Hydrodynamics. Dover Pub., 6th ed., 1945.
14. Page, Leigh: Introduction to Theoretical Physics. D. Van Nostrand Co., Inc., 1928.
15. Goldstein, Sidney: Modern Developments in Fluid Dynamics. Vol. I. Clarendon Press (Oxford), 1938.
16. Schlichting, H.: Lecture Series "Boundary Layer Theory". Part I - Laminar Flows. NACA TM 1217, 1949.
17. von Kármán, Th.: On Laminar and Turbulent Friction. NACA TM 1092, 1946.
18. Courant, R., and Friedrichs, K. O.: Supersonic Flow and Shock Waves. Interscience Pub., Inc., 1948.



$$X = \int_0^x \cos \beta \, dx + z \sin \beta$$

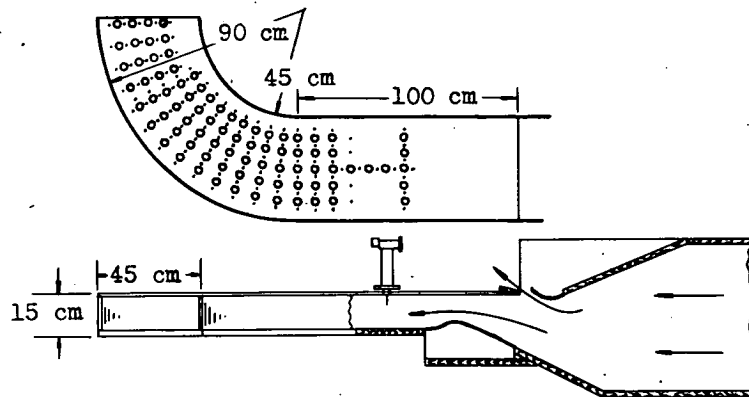
$$Y = y, \quad Z = Z_1 + z \cos \beta$$

$$Z_1 = \text{constant} - \int_0^x \sin \beta \, dx$$

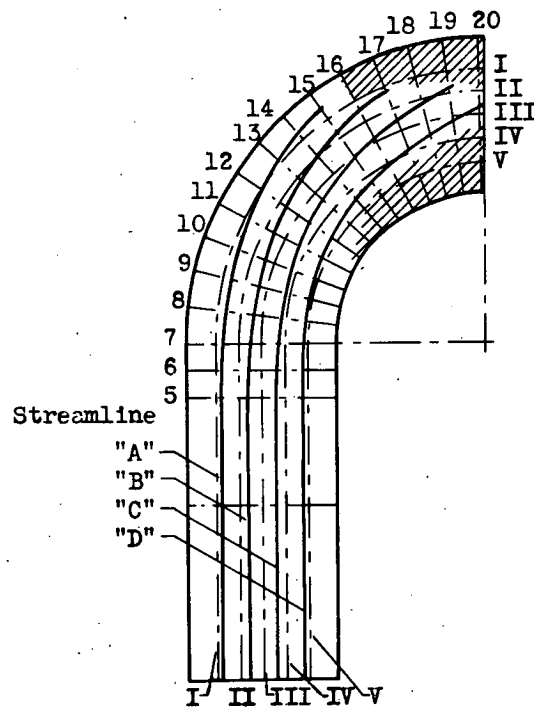
$$c = \frac{d\beta}{dx}, \quad \beta = \beta(x)$$



Figure 1. - Transformation from Cartesian coordinates  $X, Y, Z$  to orthogonal curvilinear coordinates  $x, y, z$ .



(a) Channel and measuring plate seen from below.



(b) Measuring plate seen from below, showing point and streamline designations. Shaded sections indicate regions of potential-flow breakdown.

Figure 2. - Experimental set-up of Gruschwitz (from figs. 1 and 5 of reference 9).

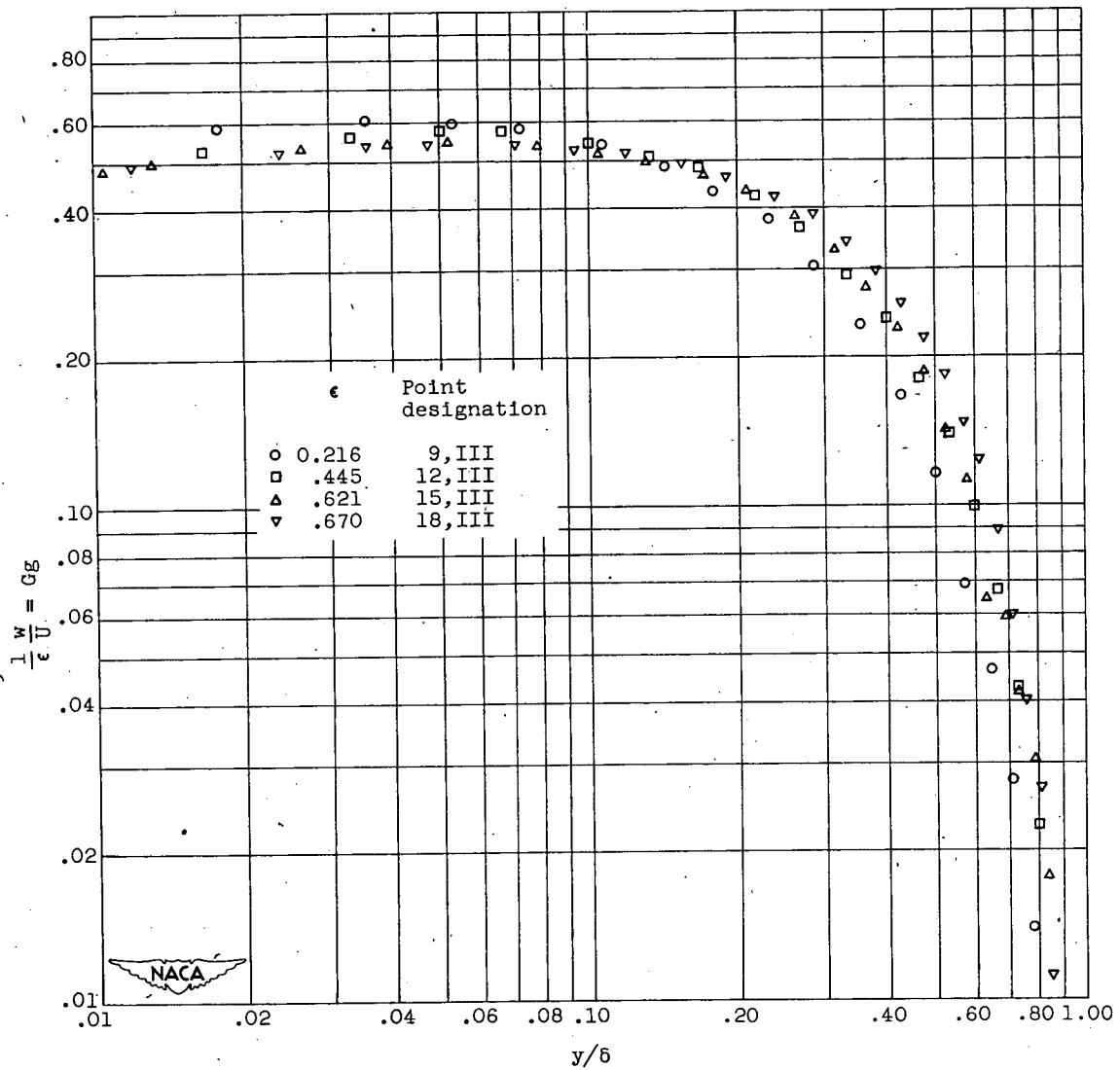
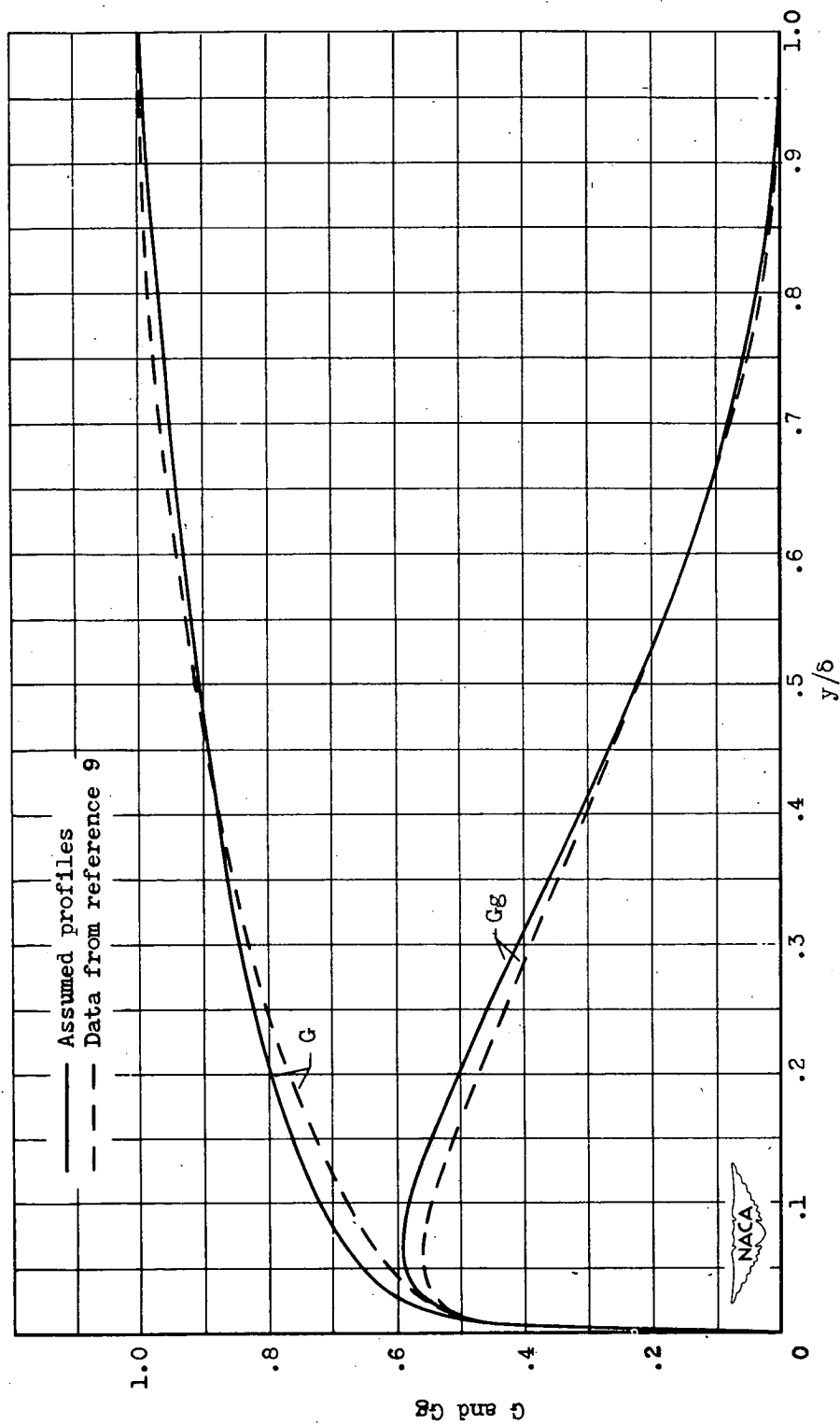
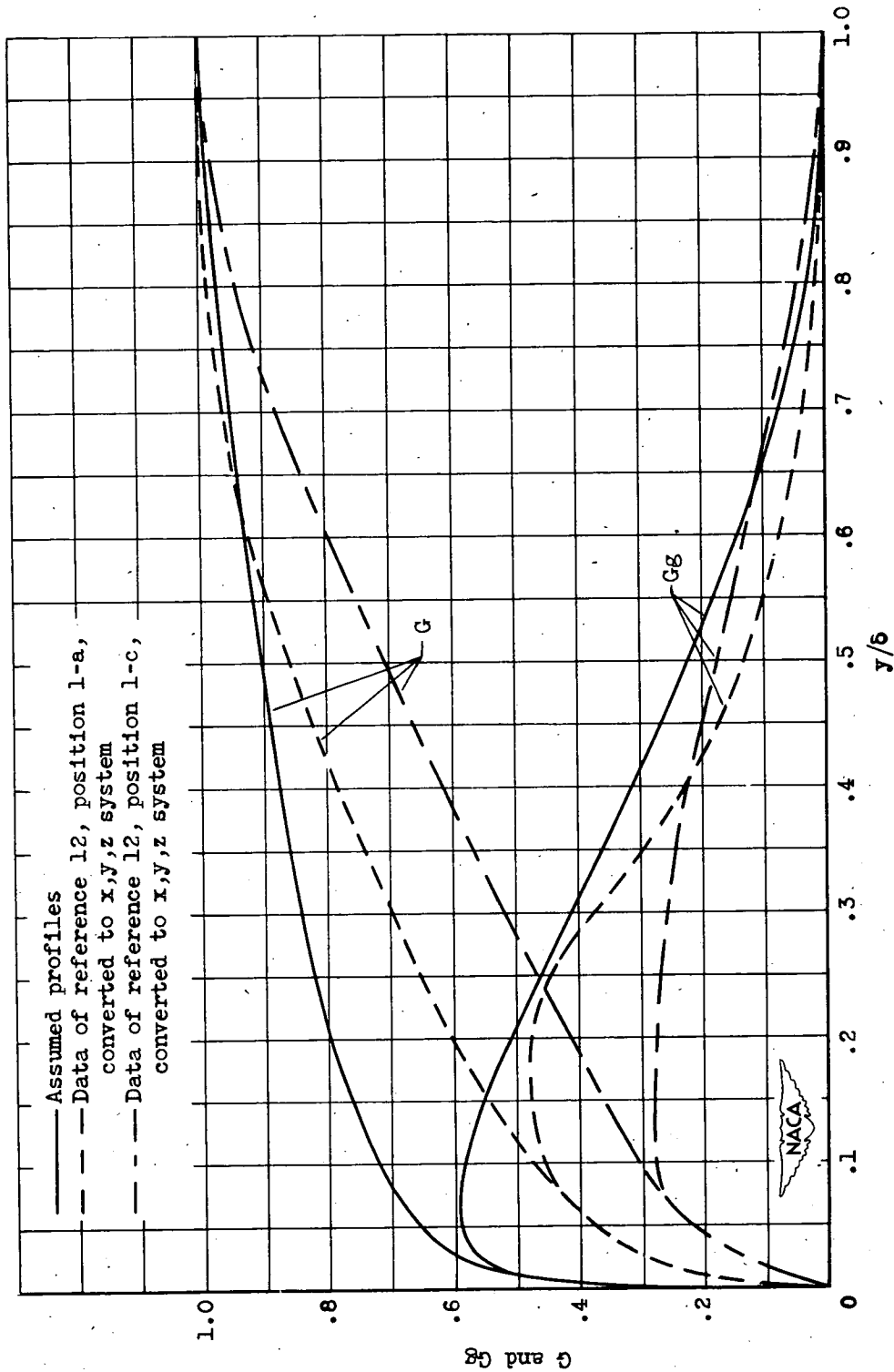


Figure 3. - Plot of  $\frac{1}{\epsilon U} Gg$  against  $\frac{y}{\delta}$  for various data from reference 9.



(a) Experimental velocity profile from reference 9 (point 15,III). Data obtained in curved duct.  $\delta = 40$  millimeters.

Figure 4. - Comparison of assumed  $G$  and  $Gg$  with experimental velocity profiles. Assumed profiles:  $G = (y/\delta)^{1/7}$ ;  $Gg = (y/\delta)^{1/7} (1-y/\delta)^2$ .



(b) Experimental velocity profile of reference 12 converted to  $x, y, z$  coordinate system. Data obtained in boundary layer of yawed wing.

Figure 4. - Concluded. Comparison of assumed  $G$  and  $Gg$  with experimental velocity profiles. Assumed profiles:  $G = (y/\delta)^{1/7}$ ;  $Gg = (y/\delta)^{1/7} (1-y/\delta)^2$ .

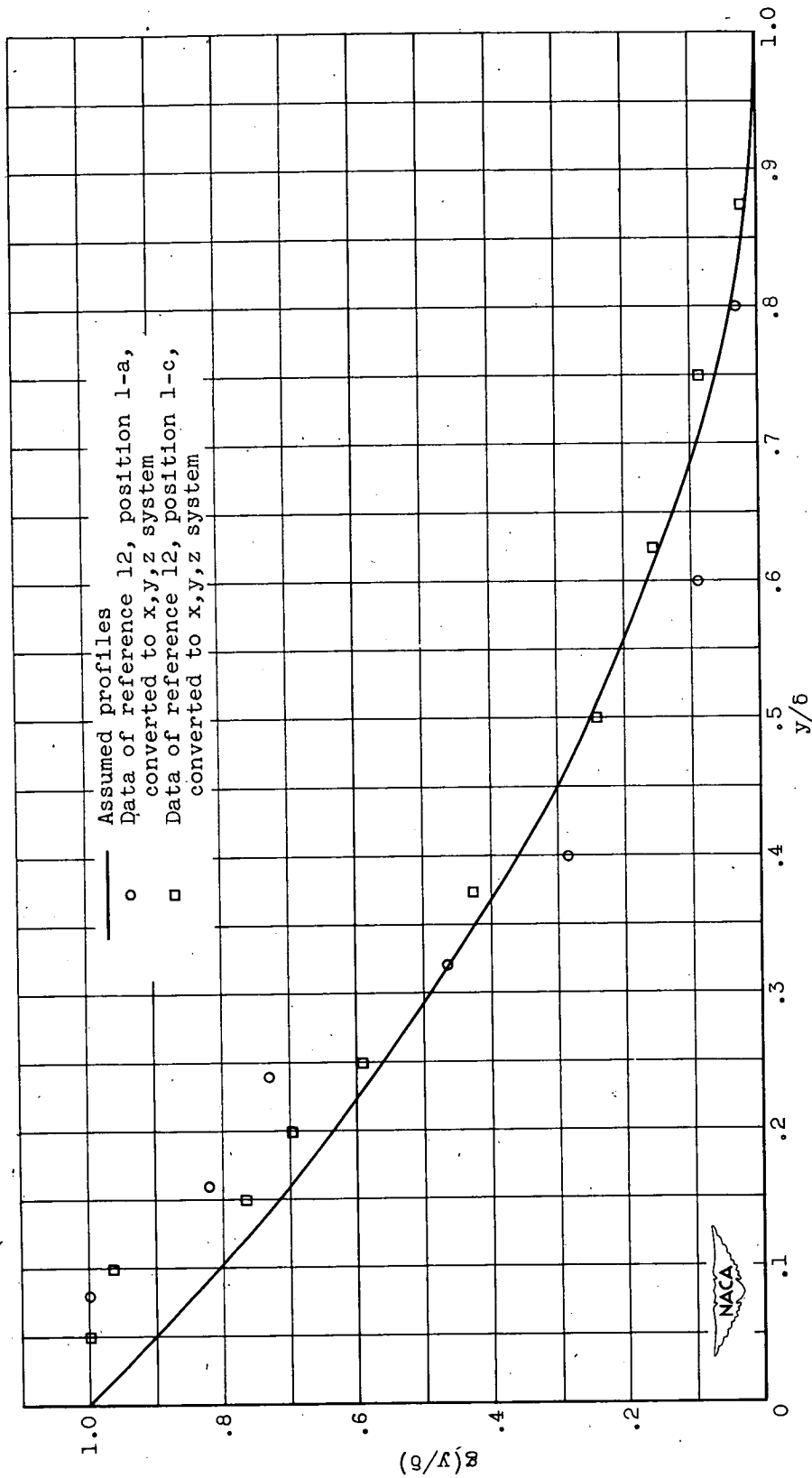
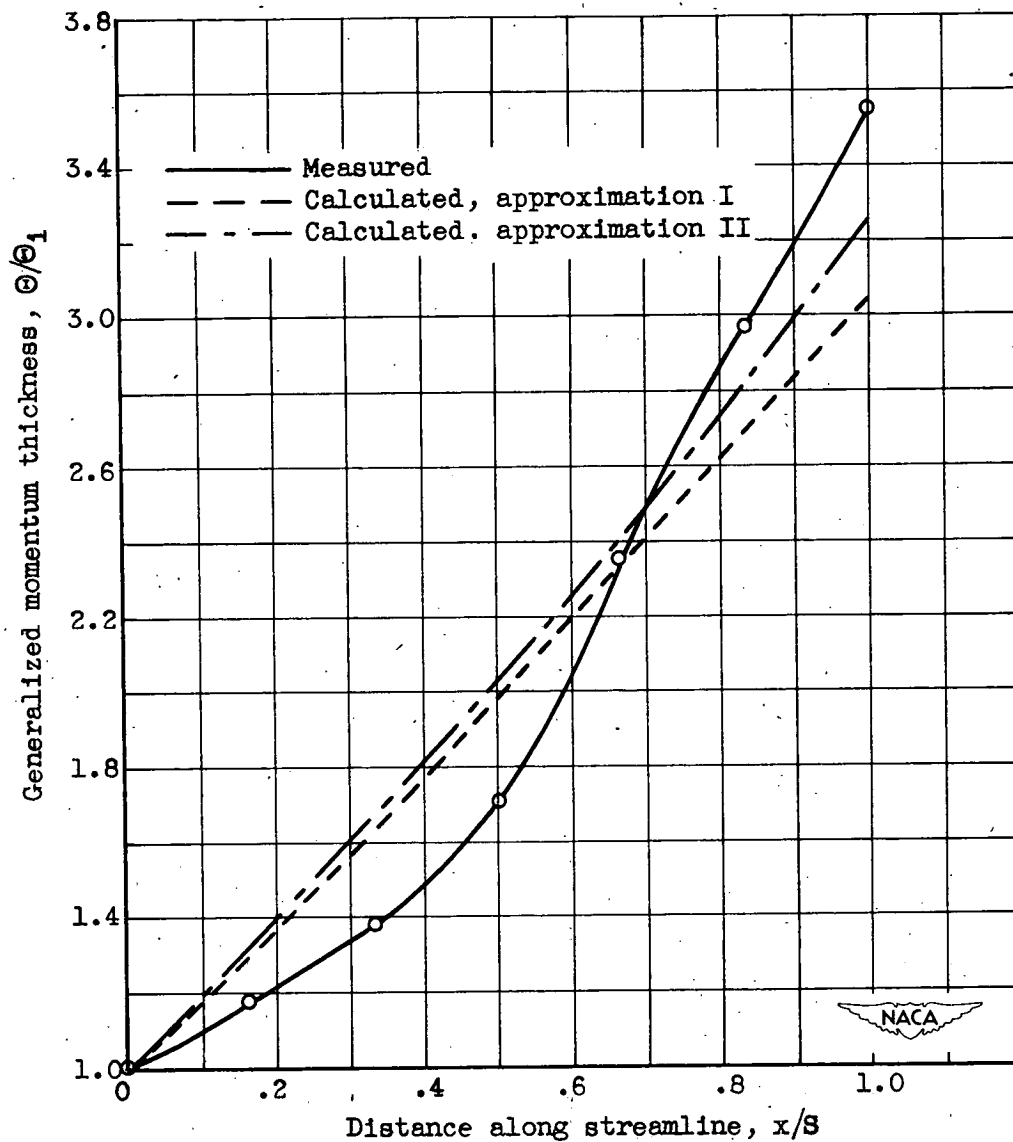


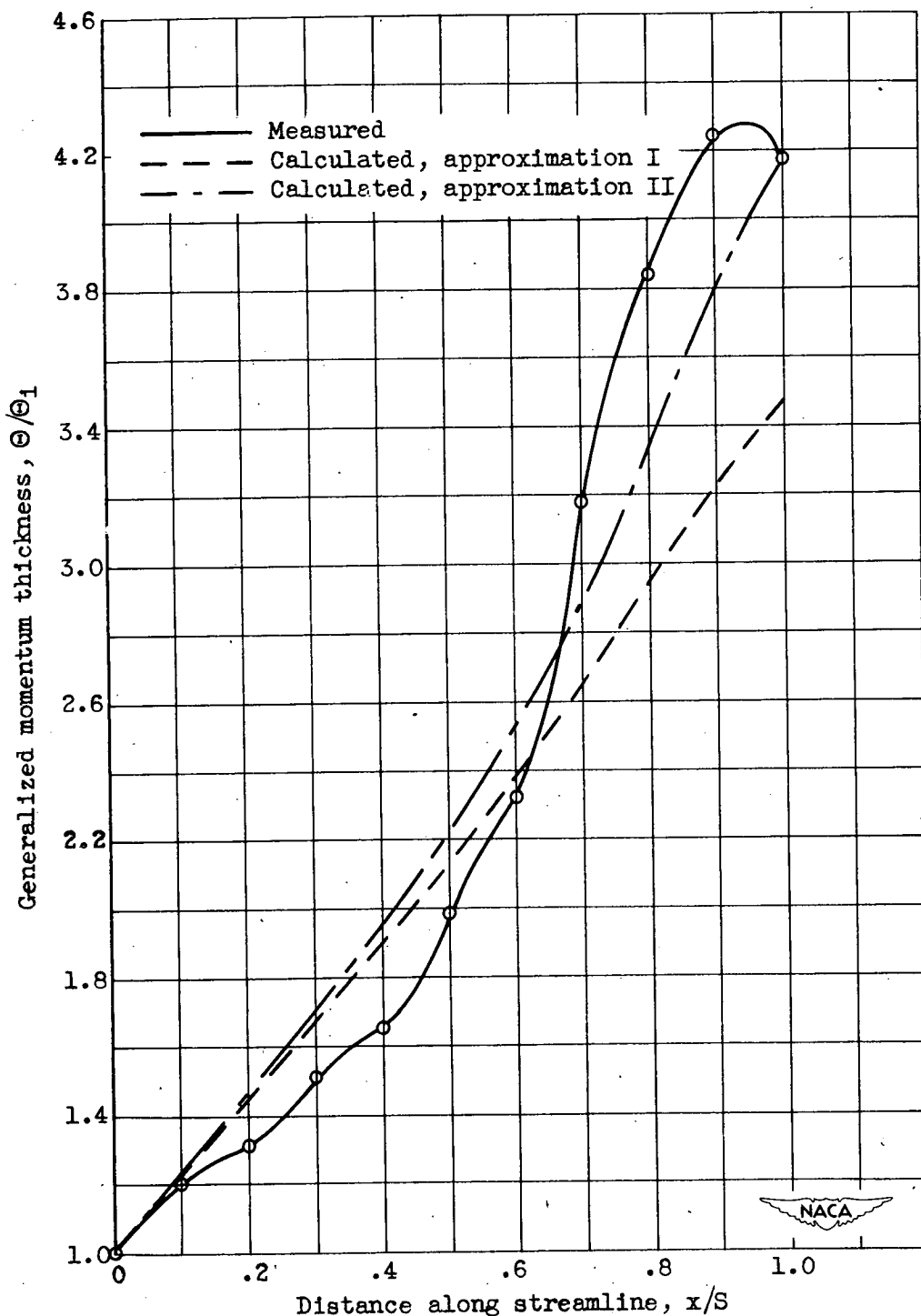
Figure 5. - Comparison of assumed correction function  $g(y/5)$  with data of reference 12 converted to x,y,z coordinate system. Assumption:  $g(y/5) = (1-y/5)^2$ .





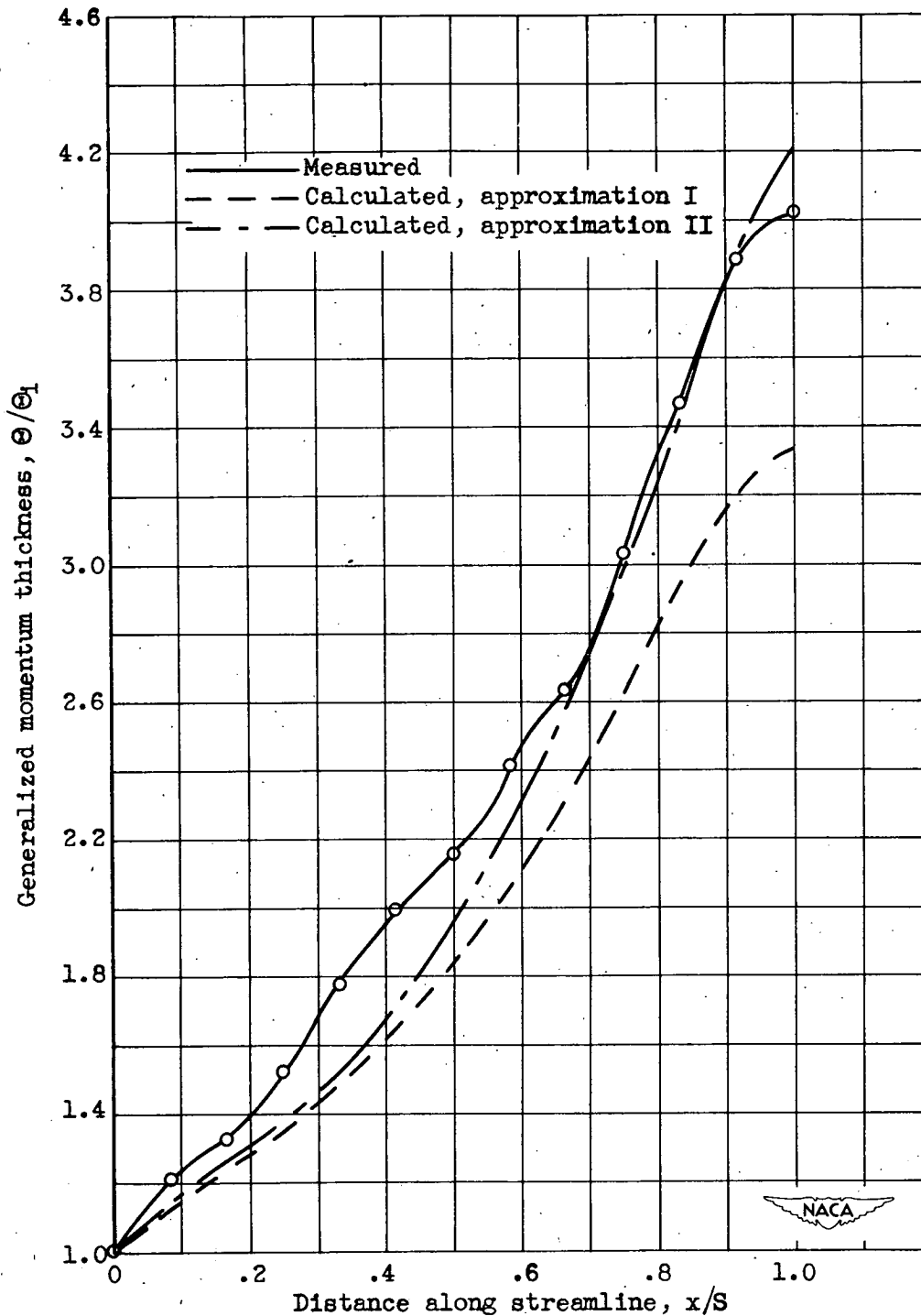
(a) Streamline "A";  $S = 22.8$  inches;  $\Theta_1 = 0.292$  inch.

Figure 6. - Comparison of calculated and measured generalized momentum thickness. Experimental data from reference 9.



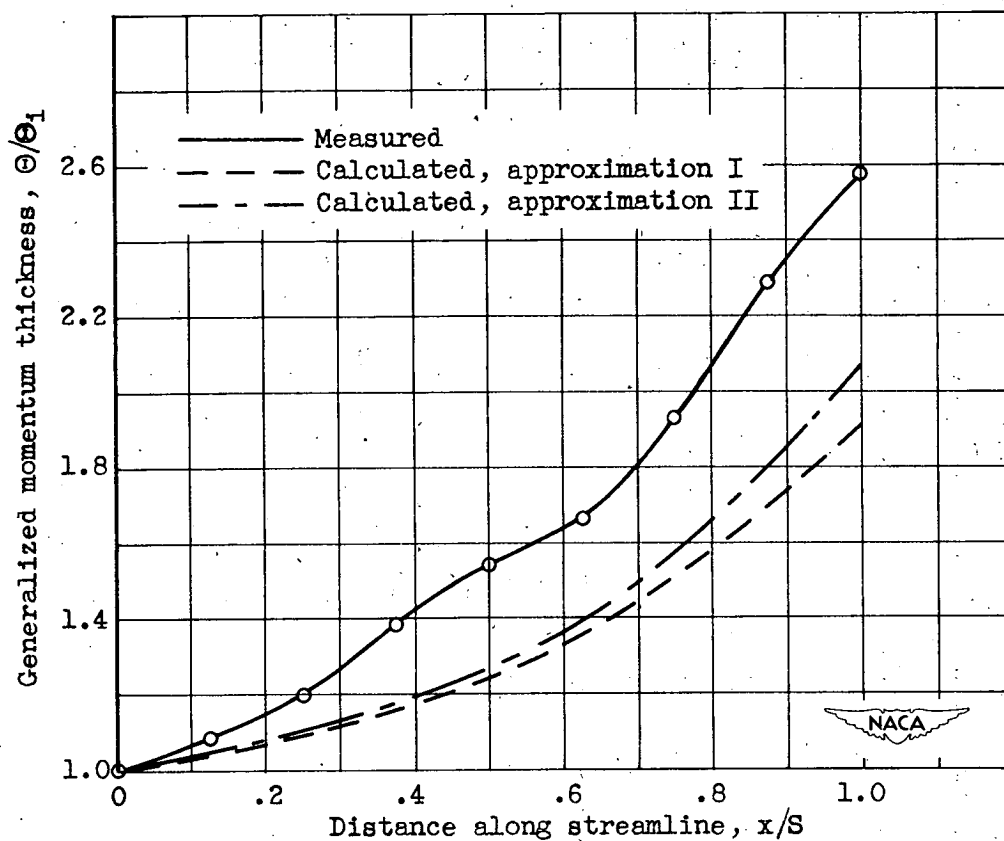
(b) Streamline "B";  $S = 34.75$  inches;  $\Theta_1 = 0.289$  inch.

Figure 6. - Continued. Comparison of calculated and measured generalized momentum thickness. Experimental data from reference 9.



(c) Streamline "C";  $S = 37.8$  inches;  $\Theta_1 = 0.286$  inch.

Figure 6. - Continued. Comparison of calculated and measured generalized momentum thickness. Experimental data from reference 9.



(d) Streamline "D";  $S = 21.25$  inches;  $\Theta_1 = 0.244$  inch.

Figure 6. - Concluded. Comparison of calculated and measured generalized momentum thickness. Experimental data from reference 9.

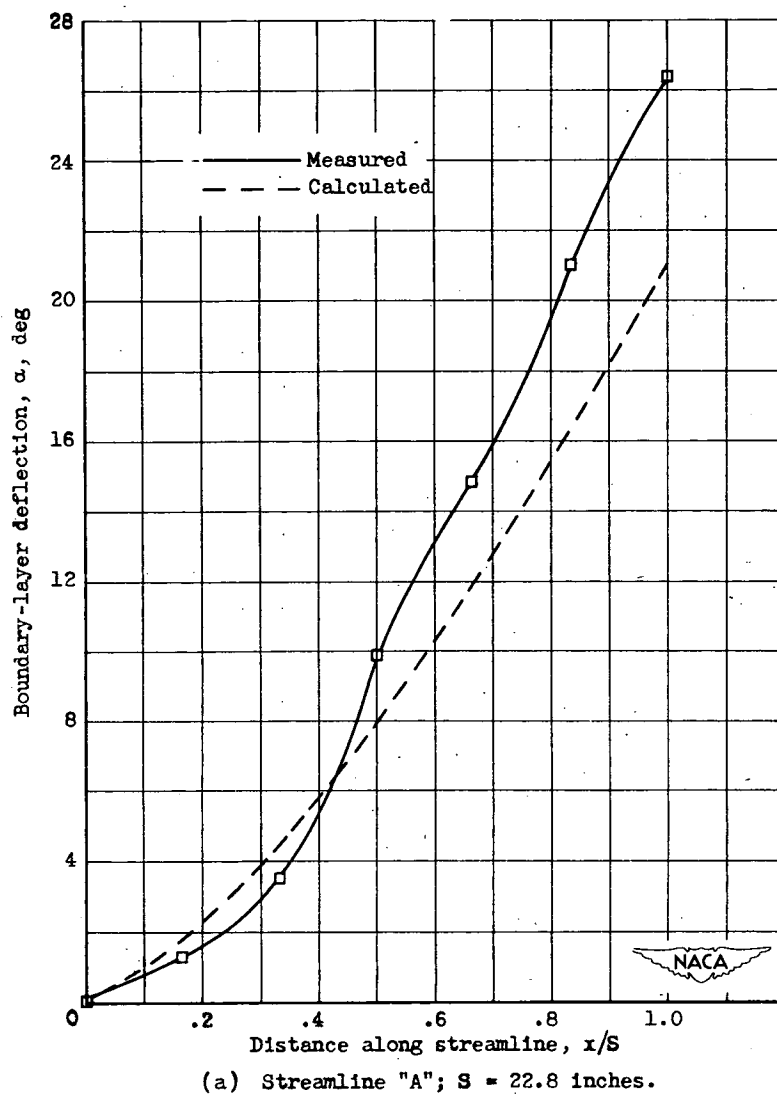
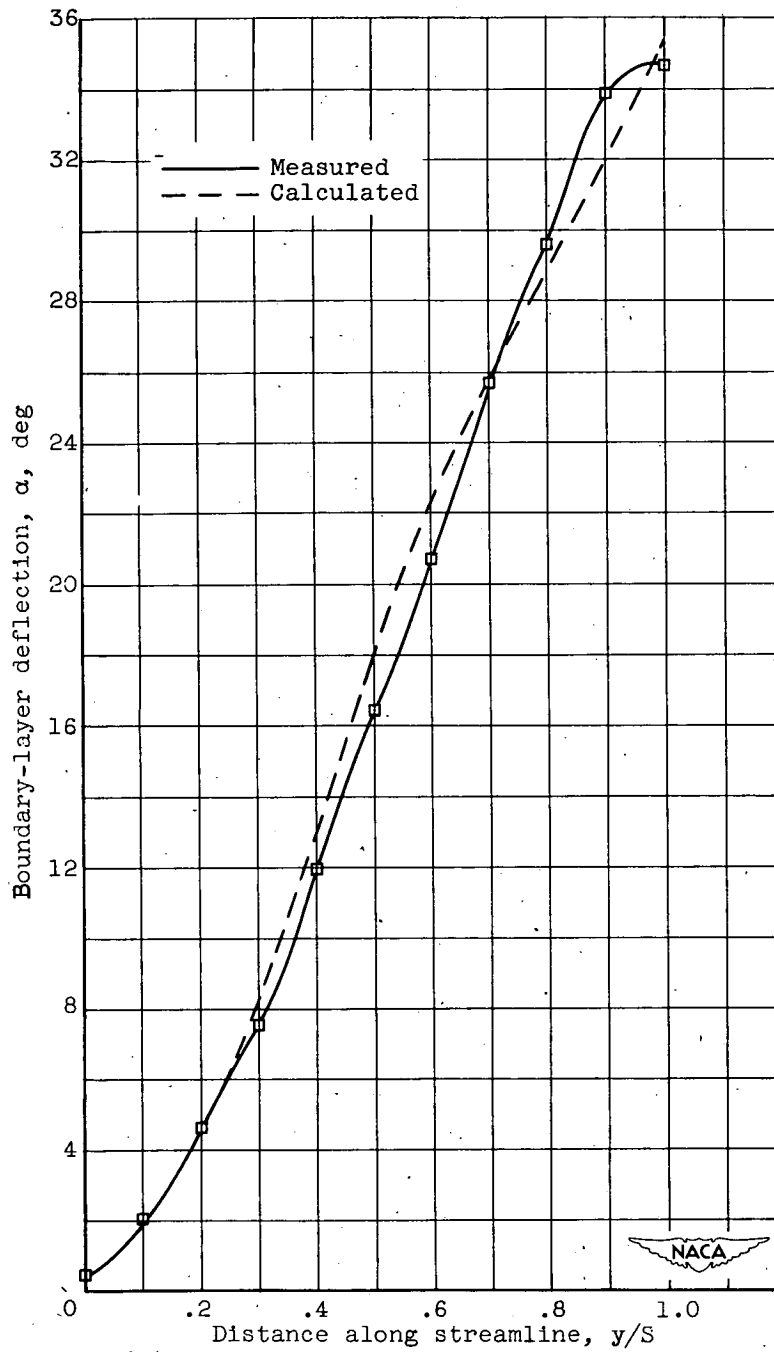


Figure 7. - Comparison of calculated and measured boundary-layer deflection at wall. Experimental data from reference 9.



(b) Streamline "B";  $S = 34.75$  inches.

Figure 7. - Continued. Comparison of calculated and measured boundary-layer deflection at wall. Experimental data from reference 9.

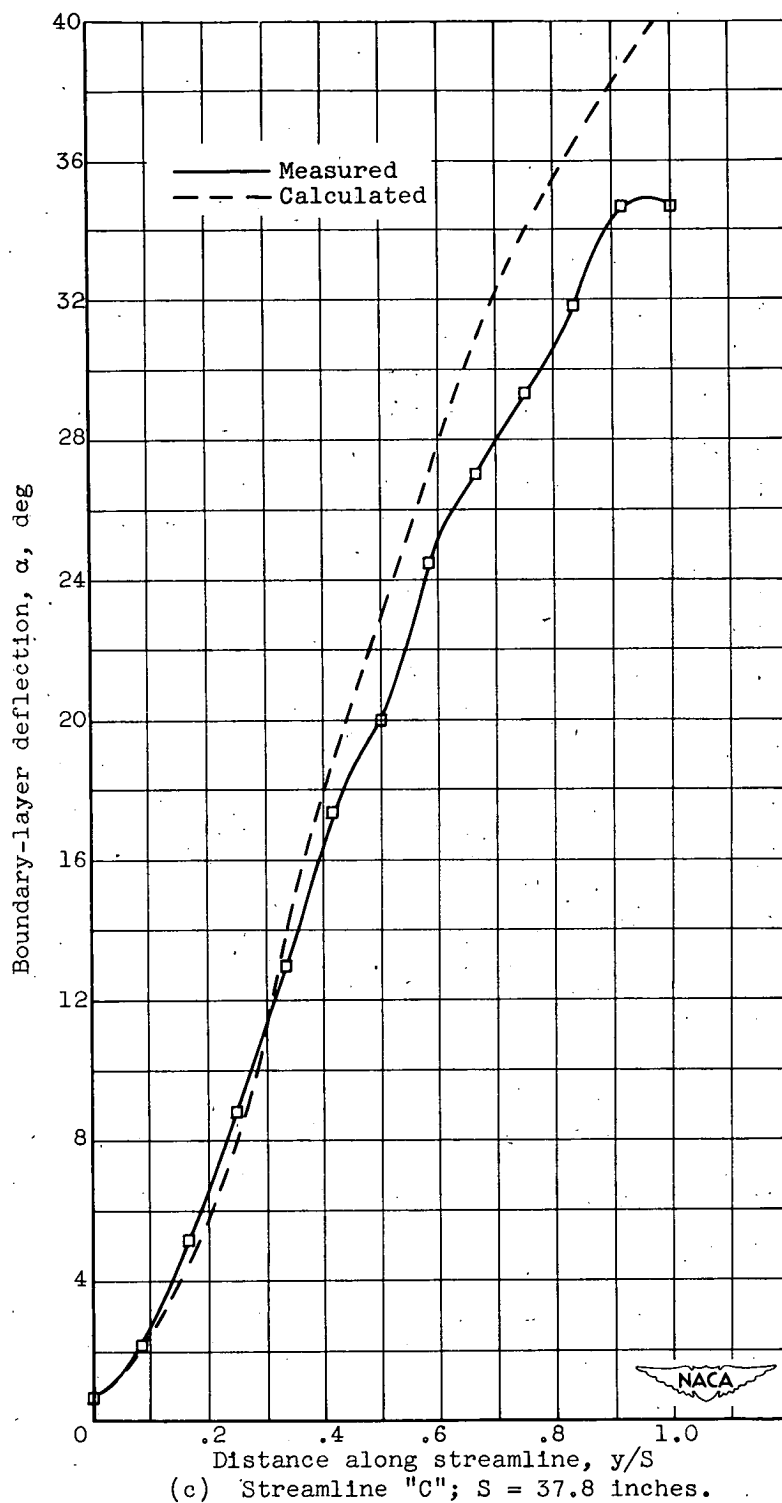
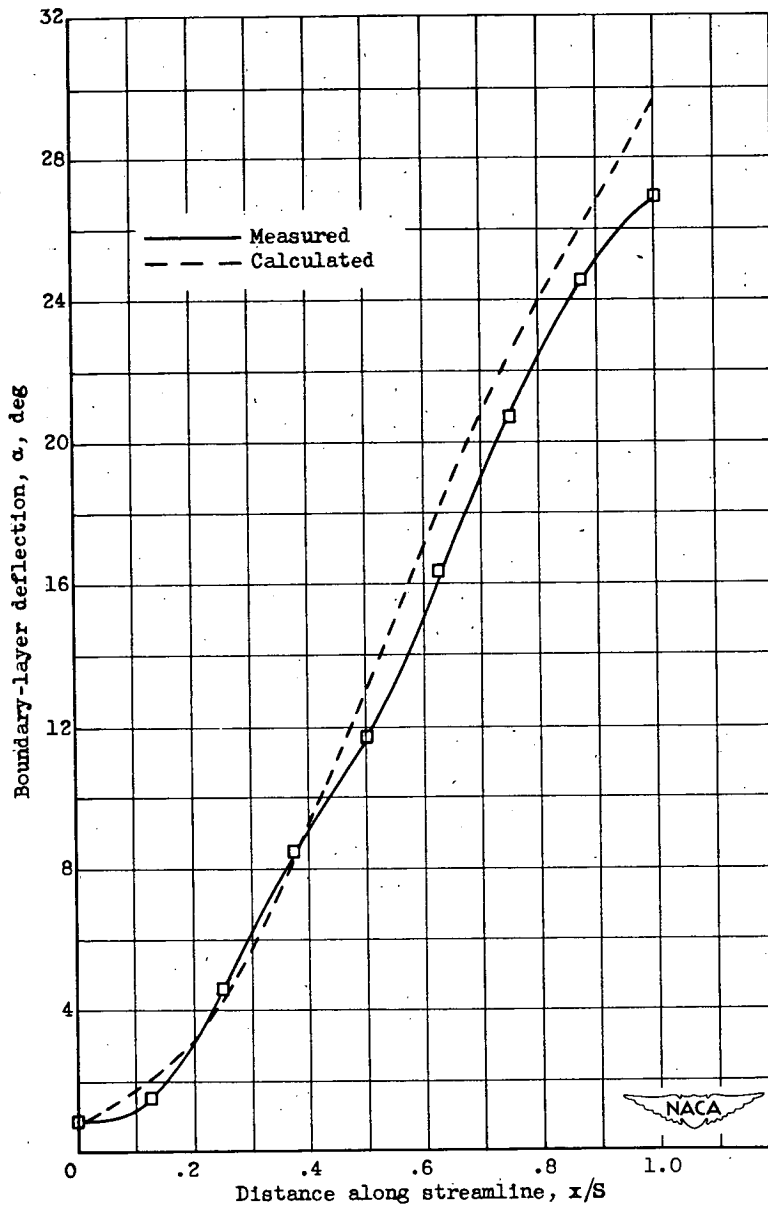


Figure 7. - Continued. Comparison of calculated and measured boundary-layer deflection at wall. Experimental data from reference 9.



(d) Streamline "D";  $S = 21.25$  inches.

Figure 7. - Concluded. Comparison of calculated and measured boundary-layer deflection at wall. Experimental data from reference 9.



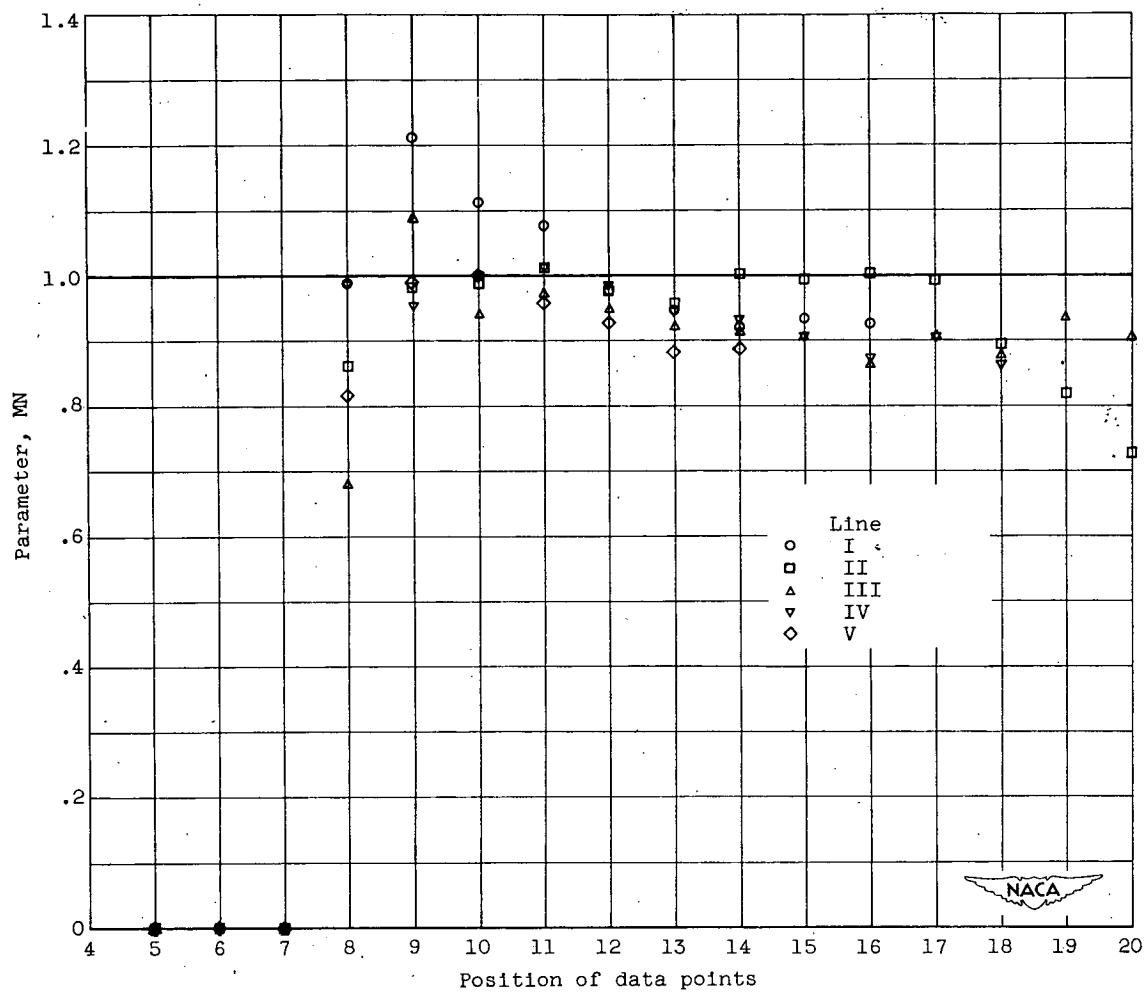


Figure 8. - Values of parameter MN for data of reference 9.